

AD-A208 386

FORMATION OF MONOLAYERS BY THE COADSORPTION OF THIOLS ON GOLD:
VARIATION IN THE LENGTH OF THE ALKYL CHAIN

C. D. Bain and G. M. Whitesides*
Department of Chemistry
Harvard University
Cambridge MA 02138

Technical Report No. 18 (May 1989)

Interim Technical Report

(Accepted for publication in J. Am. Chem. Soc.)

PREPARED FOR DEFENSE ADVANCED RESEARCH PROJECTS AGENCY
1400 Wilson Boulevard
Arlington VA 22209

DEPARTMENT OF THE NAVY
Office of Naval Research, Code 1130P
800 North Quincy Street
Arlington VA 22217-5000

ARPA Order No.: NR 356-856
Contract No.: N00014-85-K-0898
Effective Date: 85 September 01
Expiration Date: 89 May 31

Principal Investigator: George M. Whitesides
(617) 495-9430

DTIC
SELECTED
MAY 31 1989
S H D

The views and conclusions in this document are those of the authors and should not be interpreted as necessarily representing the official policies, either expressed or implied, of the Defense Advanced Research Projects Agency or the U.S. Government.

DISTRIBUTION STATEMENT A
Approved for public release;
Distribution unlimited

89 5 30 163

SECURITY CLASSIFICATION OF THIS PAGE

REPORT DOCUMENTATION PAGE

1a. REPORT SECURITY CLASSIFICATION Unclassified		1b. RESTRICTIVE MARKINGS	
2a. SECURITY CLASSIFICATION AUTHORITY		3. DISTRIBUTION / AVAILABILITY OF REPORT Approved for public release; distribution unlimited	
2b. DECLASSIFICATION / DOWNGRADING SCHEDULE			
4. PERFORMING ORGANIZATION REPORT NUMBER(S) Technical Report # 18		5. MONITORING ORGANIZATION REPORT NUMBER(S)	
6a. NAME OF PERFORMING ORGANIZATION Harvard University	6b. OFFICE SYMBOL (if applicable)	7a. NAME OF MONITORING ORGANIZATION Office of Naval Research	
6c. ADDRESS (City, State, and ZIP Code) Office of Sponsored Research Holyoke Center, Fourth Floor Cambridge MA 02138-4993		7b. ADDRESS (City, State, and ZIP Code) Code 1130P 800 North Quincy Street Arlington VA 22217-5000	
8a. NAME OF FUNDING / SPONSORING ORGANIZATION ONR/DARPA	8b. OFFICE SYMBOL (if applicable)	9. PROCUREMENT INSTRUMENT IDENTIFICATION NUMBER	
8c. ADDRESS (City, State, and ZIP Code) 800 North Quincy Street Arlington VA 22217-5000		10. SOURCE OF FUNDING NUMBERS	
		PROGRAM ELEMENT NO. 85-K-0898	PROJECT NO. NR 356-856
		TASK NO.	WORK UNIT ACCESSION NO.
11. TITLE (Include Security Classification) "Formation of Monolayers by the Coadsorption of Thiols on Gold: Variation in the Length of the Alkyl Chain"			
12. PERSONAL AUTHOR(S) C.D. Bain and G.M. Whitesides*			
13a. TYPE OF REPORT Interim	13b. TIME COVERED FROM _____ TO _____	14. DATE OF REPORT (Year, Month, Day) May 1989	15. PAGE COUNT
16. SUPPLEMENTARY NOTATION			
17. COSATI CODES		18. SUBJECT TERMS (Continue on reverse if necessary and identify by block number)	
FIELD	GROUP	SUB-GROUP	
		self-assembly, monolayers, thiols, gold, coadsorption	
19. ABSTRACT (Continue on reverse if necessary and identify by block number) Mixtures of two long-chain alkanethiols, $HS(CH_2)_nX$ and $HS(CH_2)_mY$ ($X, Y = CH_3, OH; n > m$), in which the alkyl chains have different lengths, adsorb from solution onto gold and form monolayers comprising a densely packed inner region adjacent to the gold surface and a disordered outer region in contact with the solution. When $X = Y = CH_3$ ($n \neq m$), this disordered phase makes the mixed monolayer more oleophilic than the ordered, pure (i.e., single-component) monolayers. When $X = Y = OH$, the pure monolayers are wet by water, but the mixed monolayers are less hydrophilic because nonpolar polymethylene chains are exposed at the surface. When $X = CH_3, Y = OH$ ($n = 21, m = 11$), a very sharp transition occurs from a monolayer composed largely of the longer, methyl-terminated component to the shorter, hydroxyl-terminated component as the mole fraction of $HS(CH_2)_{11}OH$ in the adsorption solution is increased. From solutions containing two thiols, adsorption of the thiol with the longer chain			
20. DISTRIBUTION / AVAILABILITY OF ABSTRACT <input checked="" type="checkbox"/> UNCLASSIFIED UNLIMITED <input type="checkbox"/> SAME AS RPT <input type="checkbox"/> DTIC USERS		21. ABSTRACT SECURITY CLASSIFICATION	
22a. NAME OF RESPONSIBLE INDIVIDUAL Dr. Joanne Milliken		22b. TELEPHONE (Include Area Code)	22c. OFFICE SYMBOL

10-11-68

is preferred. This preference is greater when the monolayers are adsorbed from ethanol than from isooctane. The mixed monolayers do not act as ideal two-dimensional solutions. The adsorption isotherms suggest a positive excess free energy of mixing of the two components in the monolayer. The compositions of the monolayers appear to be determined largely by thermodynamics, although in some cases there is also a kinetic contribution to the composition. The two components in mixed monolayers do not phase-segregate into macroscopic islands (greater than a few tens of angstroms across) but are probably not randomly dispersed within the monolayer. The wettability of mixed, methyl-terminated monolayers can be partially rationalized by the geometric mean methyl-terminated monolayers can be partially rationalized by the geometric mean approximation, but a full description probably requires inclusion of the entropy of mixing at the monolayer-liquid interface. The hysteresis in the contact angle on these monolayers cannot be explained by theories of wetting based on macroscopic heterogeneity. Contact angles are more sensitive than optical ellipsometry or X-ray photoelectron spectroscopy to certain types of changes in the composition and structure of these monolayers.

(Fuji)

Accession For	
NTIS GRA&I	<input checked="" type="checkbox"/>
DTIC TAB	<input type="checkbox"/>
Unannounced	<input type="checkbox"/>
Justification	
By	
Distribution/	
Availability Codes	
Dist	Avail and/or Special
A-1	



**Formation of Monolayers by the Coadsorption of Thiols on Gold: Variation in
the Length of the Alkyl Chain¹**

Colin D. Bain² and George M. Whitesides*

Department of Chemistry,

Harvard University,

Cambridge, Massachusetts 02138

Abstract

Mixtures of two long-chain alkanethiols, $\text{HS}(\text{CH}_2)_n\text{X}$ and $\text{HS}(\text{CH}_2)_m\text{Y}$ ($\text{X}, \text{Y} = \text{CH}_3, \text{OH}; n > m$), in which the alkyl chains have different lengths, adsorb from solution onto gold and form monolayers comprising a densely packed inner region adjacent to the gold surface and a disordered outer region in contact with the solution. When $\text{X} = \text{Y} = \text{CH}_3$ ($n \neq m$), this disordered phase makes the "mixed monolayer" more oleophilic than the ordered, pure (i.e. single-component) monolayers. When $\text{X} = \text{Y} = \text{OH}$, the pure monolayers are wet by water, but the mixed monolayers are less hydrophilic because nonpolar polymethylene chains are exposed at the surface. When $\text{X} = \text{CH}_3, \text{Y} = \text{OH}$ ($n = 21, m = 11$), a very sharp transition occurs from a monolayer composed largely of the longer, methyl-terminated component to the shorter, hydroxyl-terminated component as the mole fraction of $\text{HS}(\text{CH}_2)_{11}\text{OH}$ in the adsorption solution is increased. From solutions containing two thiols, adsorption of the thiol with the longer chain is preferred. This preference is greater when the monolayers are adsorbed from ethanol than from isooctane. The mixed monolayers do not act as ideal two-dimensional solutions. The adsorption isotherms suggest a positive excess free energy of mixing of the two components in the monolayer. The compositions of the monolayers appear to be determined largely by thermodynamics, although in some cases there is also a kinetic contribution to the composition. The two components in mixed monolayers do not phase-segregate into macroscopic islands (greater than a few tens of angstroms across) but are probably not randomly dispersed within the monolayer. The wettability of mixed, methyl-terminated monolayers can be partially rationalized by the geometric mean approximation, but a full description probably requires inclusion of the entropy of mixing at the monolayer-liquid interface. The hysteresis in the contact angle on these monolayers cannot be explained by theories of wetting based on macroscopic heterogeneity. Contact angles are more sensitive than optical ellipsometry or X-ray photoelectron spectroscopy to certain types of changes in

the composition and structure of these monolayers.

Introduction

Long-chain alkanethiols, $\text{HS}(\text{CH}_2)_n\text{X}$, adsorb from solution onto gold and form densely packed monolayer films.^{3,4} This paper is the second of two that present studies of the "mixed monolayers" formed by the coadsorption of two thiols. In the preceding paper in this issue,⁵ we discussed the influence of the tail group, X, and the nature of the solvent on the formation of monolayer films on gold and on the properties of the resulting surfaces. In this paper, we turn our attention to monolayers formed by coadsorption of two thiols that differ in the length, n , of the polymethylene chain.

We present data here for mixed monolayers in three general classes: (a) both the thiol with the longer chain and the thiol with the shorter chain are terminated by methyl groups ($\text{X} = \text{CH}_3$); (b) both thiols are terminated by hydroxyl groups ($\text{X} = \text{OH}$);⁶ (c) a long-chain thiol is terminated by a methyl group and a short-chain thiol is terminated by a hydroxyl group.⁷ We have previously published preliminary results from the latter two systems as communications.^{6,7}

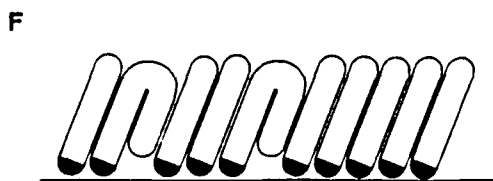
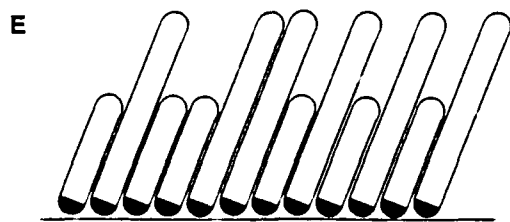
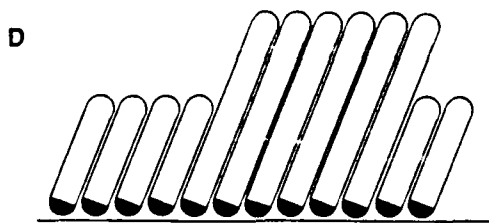
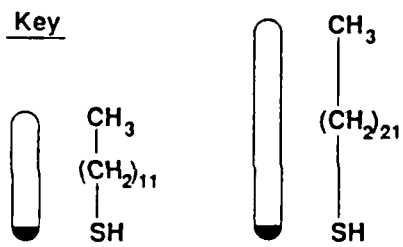
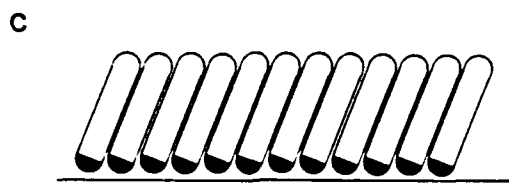
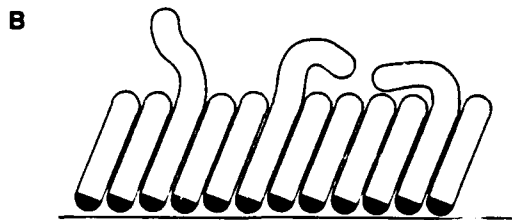
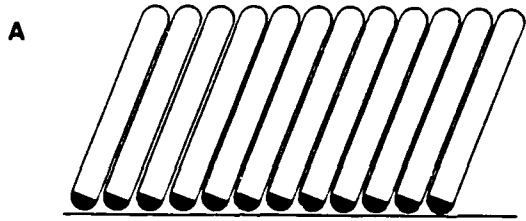
We had three broad aims in this study. First, we wished to understand how the composition of the monolayer was related to the concentrations of the thiols in solution. One of the key questions is whether the molecular constituents (probably alkyl thiolates, RS^-) of the monolayer are in thermodynamic equilibrium with their precursors (alkanethiols) in solution, or whether the kinetics of adsorption determine the composition of the monolayer. If the monolayers are in thermodynamic equilibrium with the adsorption solutions, then it should be possible to derive thermodynamic properties of the monolayers from the adsorption isotherms. A quantitative analysis of the adsorption isotherms is beyond the scope of this paper. Here we discuss qualitatively the impact of excess entropy and enthalpy on the composition of the monolayers.⁸

Second, we wished to elucidate the structure of the mixed monolayers. In particular, we wanted to establish whether the two components in the monolayer segregate

into macroscopic, single-component domains, and, if not, to what extent the components do aggregate into small clusters on the surface. In this context we use "macroscopic" to mean sufficiently large that the properties of the monolayer are dominated by molecules that are in an environment indistinguishable from that in a pure (i.e. single-component) monolayer. In the absence of long-range electrostatic interactions, macroscopic probably applies to islands more than a few tens of angstroms across. To address this problem we used inferential evidence from contact angles (θ), X-ray photoelectron spectroscopy (XPS) and ellipsometry. We have not attempted to determine the pair correlation function of the components within the monolayer directly by scattering experiments.

Third, we wished to investigate the macroscopic physical properties -- particularly the wettability -- of interfaces that can be generated with mixed monolayers of thiols on gold. The properties of mixed monolayers are closely related to their structure. Long-chain thiols form well-packed, oriented monolayers on gold in which the hydrocarbon chains are canted $\sim 30^\circ$ from the normal to the surface (Figure 1A and 1C).^{4,9} Methyl-terminated thiols generate surfaces that are composed of densely packed methyl groups and are both hydrophobic ($\theta_a(\text{H}_2\text{O}) = 112^\circ$) and oleophobic ($\theta_a(\text{HD}) = 47^\circ$; HD = hexadecane).³ Hydroxyl-terminated thiols form monolayers that are wet by both hexadecane and water ($\theta_a(\text{H}_2\text{O}) = \theta_a(\text{HD}) \sim 0^\circ$).⁶ If two thiols with the same tail group but different chain lengths were to separate into discrete macroscopic islands, then the wettability of the mixed monolayers would be the same as that of the pure monolayers (Figure 1D). A more interesting situation would arise if the two components were dispersed on a molecular scale: the lower part of the monolayer, adjacent to the gold surface, would still be well-packed;¹⁰ the upper part would be disordered and liquid-like (Figure 1B). The presence of this disordered phase would be evident as a large deviation in the contact angles from the values observed on the pure monolayers. If the both thiols were terminated by hydroxyl groups, the nonpolar methylene groups exposed in the mixed monolayers would raise the contact angle of water relative to the pure monolayers. If both

Figure 1. Schematic illustration of monolayers of thiols on gold. (A) Pure monolayer of docosanethiol. (B) Mixed monolayer of docosanethiol and dodecanethiol near the composition that yielded the lowest contact angles with hexadecane. (C) Pure monolayer of dodecanethiol. (D), (E), (F) Structures that we believe do not occur in the monolayers studied here. (D) Mixtures of docosanethiol and dodecanethiol phase-separated into islands that have the properties of the pure monolayers are not consistent with the observed contact angles. (E) An oriented monolayer with the two components dispersed on a molecular scale is unstable relative to (B). (F) Hairpin loops in the thiol with the longer chain are energetically unstable with respect to incorporation of additional molecules of a thiol into the monolayer.



thiols were terminated by methyl groups, the surface of the mixed monolayers would resemble a liquid hydrocarbon. Since any liquid spreads on a surface composed of the same liquid, we would expect the contact angle with hexadecane to exhibit a much lower contact angle on the mixed monolayers than on the pure monolayers.

The data that we present in this paper can be understood if the compositions of the monolayers are at, or near, their values at equilibrium with the solutions from which they were adsorbed. We discussed in the preceding paper the apparent contradiction between thermodynamic control over the adsorption process and the slow rate of exchange between the components in fully formed monolayers and thiols in solution. The resolution of this problem may lie in rapid equilibration early in the adsorption process, possibly through a physisorbed thiol, although we have no proven mechanism for such equilibration. The composition of the fully formed monolayer would be the result of kinetic trapping of the composition of the equilibrating monolayer early in the adsorption process. The compositions of some of the monolayers studied in this paper did vary slowly with time, indicating that the kinetics of adsorption played a more important role than in the thinner monolayers discussed in the preceding paper. Equilibration between the monolayer and the solution may have slowed down before the equilibrium composition had been reached in these monolayers. For none of the monolayers were we able to rationalize the observed compositions purely on the basis of kinetics. The available evidence also points to the absence of macroscopic islands caused by phase-segregation of the two components within the monolayer. We will present the data in this paper under the assumptions that thermodynamics controls the composition of the mixed monolayers and that the monolayers are not phase-segregated, and then discuss the evidence that lends support to these assumptions. We will also try to define more closely the extent of aggregation of the two components in the monolayer.

By using monolayers containing chains of different length we can control the degree of disorder at interfaces and vary the structure perpendicular to the surface. There

are many reasons for interest in such systems. By relating the contact angle and the hysteresis in the contact angle to the structure of a surface we can test theories of wetting.^{11,12,13,14} Current theories of wetting are based on the consideration of the enthalpy of intermolecular interactions and do not specifically include the interfacial entropy except in so far as it scales with the enthalpy. Specifically, current theories do not incorporate entropy of mixing at the solid-liquid interface. Since the variation in the degree of order at a solid-liquid interface changes the interfacial entropy, any model that seeks to provide a full description of wetting in these systems will have to address the role of entropy. We also attempt to reconcile the hysteresis observed in the contact angle with the predictions of theories based on macroscopic heterogeneity, and conclude that hysteresis in these systems is determined by the microscopic structure of the surface.

Mixed monolayers containing components of different chain lengths could potentially be used to construct cavities of a controlled size containing specific functional groups.¹⁵ Such systems would be useful for modelling enzyme activity, molecular recognition, heterogeneous catalysis and electrode processes. Control over the tail groups exposed at the monolayer-liquid interface permits the study of the effect of environment on acidity/basicity and chemical reactivity at interfaces. The mixed methyl-terminated chains provide a model system for synthetic membranes incorporating lipids of mixed chain lengths.¹⁶ Direct applications also exist in the modification of wetting and adhesion, in chromatography,¹⁷ and perhaps in electronic devices.

Recently there has been much interest in the measurement of intermolecular interactions with Tabor force balances.¹⁸ Atomically smooth gold films can be formed on mica plates of the type normally used in force balance measurements.¹⁹ Monolayers on gold are more densely packed than monolayers of ammonium salts on mica,²⁰ and, as we show in these papers, offer great flexibility over the structure at the monolayer-liquid interface. In addition, monolayers of thiols on gold should prevent the leaching of ions from the mica into solution,²¹ thus eliminating the effects of the electrostatic double layer.

The general strategy in this paper, as in the preceding paper, was to adsorb monolayers onto gold from solutions containing two thiols at various mole fractions but with a fixed total concentration of thiol moieties. We then used ellipsometry and XPS to determine the composition of the monolayer and contact angles to measure its wettability. Contact angles also provide structural information about the surface of a monolayer. The contact angle of water is sensitive to the polarity of the surface; the contact angle of hexadecane reflects the polarizability and, as we shall see, the degree of order in the surface. The contact angle of water is more sensitive than the contact angle of hexadecane to the presence of polar functional groups buried below the monolayer-liquid interface.²² A comparison of the contact angles of water and hexadecane can thus provide considerable insight into the three-dimensional structure of a monolayer. Hysteresis in the contact angle probably also carries valuable structural information, but we do not yet understand how to interpret hysteresis.

In this paper we will use terms such as "monolayer of alkanethiol" to specify the precursor from which the monolayer was formed, even though the actual species on the surface is probably an alkyl thiolate (RS^-).^{3,23} We will also use terms such as "methyl surface" to refer to the surface of a monolayer that exposes primarily methyl groups at the monolayer-air or monolayer-liquid interfaces. We define a parameter, R , to be the ratio *in solution* of the concentration of the species with the shorter chain to the species with the longer chain: $R = [\text{HS}(\text{CH}_2)_m\text{Y}]_{\text{sol}}/[\text{HS}(\text{CH}_2)_n\text{X}]_{\text{sol}}$ ($m < n$). Contact angles are plotted with axes that are linear in $\cos \theta$, not in θ itself. $\cos \theta$ is related to surface free energies through Young's equation²⁴

$$\gamma_{\text{lv}} \cos \theta = \gamma_{\text{sv}} - \gamma_{\text{sl}} \quad (1)$$

where γ_{lv} , γ_{sv} , and γ_{sl} are the liquid-vapor, solid-vapor, and solid-liquid surface free energies, respectively. Changes in $\cos \theta$ are thus linearly related to changes in interfacial

free energies. In this paper we express the hysteresis in the contact angle as the difference between the minimum receding contact angle and the advancing contact angle, expressed as cosines: $\cos \theta_r - \cos \theta_a$.²⁵

Experimental Section

Details of the purification and synthesis of the materials used in these studies and general description of procedures have been provided in the preceding paper.⁵

Both ellipsometric thicknesses and XPS intensities were used to calculate the composition of monolayers containing two components with different chain lengths. The ellipsometric readings were converted to compositions on the assumption that the ellipsometric thickness is a linear function of the composition. There is no *a priori* reason why this assumption should be valid, since the optical constants of the mixed monolayers might differ from those of the pure monolayers. Radiotracer measurements on partial monolayers of octadecylamine on chromium²⁶ supported a linear relationship, however, so our approximation is probably valid.

The compositions of monolayers comprising two methyl-terminated thiols were calculated from the ratio of the intensities of the C(1s) and Au(4f_{7/2}) photoelectrons. If the monolayers are homogeneous (i.e. they do not comprise single-component domains) the C/Au ratio is given to a good approximation by²⁷

$$\frac{C}{Au} = \frac{C_{\infty}(1 - e^{-d/\lambda_1 \sin \theta})}{Au_0 e^{-d/\lambda_2 \sin \theta}} \quad (2)$$

where C_{∞} = C(1s) intensity from an infinitely thick monolayer of an alkanethiol on gold

Au_0 = Au(4f_{7/2}) intensity from a clean gold surface

θ = the angle between the axis of the analyzer and the surface horizontal (the take-

off angle)

λ_1 = attenuation length of C(1s) photoelectrons in a hydrocarbon film ($\sim 36 \text{ \AA}$)

λ_2 = attenuation length of Au(4f_{7/2}) photoelectrons in a hydrocarbon film ($\sim 42 \text{ \AA}$)

d = thickness of the monolayer

We could use this formula directly to calculate the thickness, and hence the composition of the monolayers. In practice, it is easier to calibrate the C/Au ratio against actual monolayers of pure alkanethiols with various chain lengths. The C/Au ratios from the mixed monolayers shown in Fig. 4 were compared with the C/Au ratio obtained from pure monolayers of HS(CH₂)_{*n*}CH₃ adsorbed from ethanol.²³ Since the acquisition parameters were different in the two experiments, the ratios were normalized to the same value of C/Au for monolayers of HS(CH₂)₁₁CH₃. With this normalization, the C/Au ratio for the pure monolayer of HS(CH₂)₂₁CH₃ adsorbed from isooctane corresponded to a monolayer 21.5 carbons thick adsorbed from ethanol. For each mixed monolayer we determined an *equivalent chain length* of a pure monolayer of an alkanethiol on gold. Finally, we calculated the composition of the monolayer on the assumption that the composition was a linear function of the equivalent chain length, i.e. that attenuation of the photoelectrons is determined only by the mass of the hydrocarbon film per unit surface area and not by the structure of the film.

Results

HS(CH₂)₂₁CH₃ + HS(CH₂)_{*n*}CH₃ Adsorbed from Ethanol. We initially attempted to form mixed monolayers containing two methyl-terminated thiols of different chain lengths by adsorbing monolayers onto gold from 1:1 mixtures of HS(CH₂)₂₁CH₃ and HS(CH₂)_{*n*}CH₃ ($n = 6 - 18$) in ethanol. All the monolayers were autophobic and the ellipsometric thickness of the monolayers (Figure 2) was constant, independent of the value of n . The dotted line in Figure 2 shows the thicknesses expected if the compositions of the

solution and the monolayer were the same. The observed data indicate the formation of pure monolayers of $\text{HS}(\text{CH}_2)_{21}\text{CH}_3$ with no incorporation of the shorter component that was detectable by ellipsometry. We note that if the formation of the monolayer were under kinetic control (for example, limited by the rate of diffusion of thiols to the surface) we would expect the thicknesses to fall below the dotted line in Fig. 2, not above it.

$\text{HS}(\text{CH}_2)_{21}\text{CH}_3 + \text{HS}(\text{CH}_2)_{11}\text{CH}_3$ Adsorbed from Ethanol. From Fig. 2 it is clear that to form mixed monolayers of different chain lengths from ethanol, we must use mass action to drive the incorporation of the shorter chain into the monolayer. Figure 3 shows the ellipsometric thickness and the advancing contact angle of hexadecane (HD) on monolayers adsorbed from ethanolic solutions containing $\text{HS}(\text{CH}_2)_{21}\text{CH}_3$ and $\text{HS}(\text{CH}_2)_{11}\text{CH}_3$ in the ratio $R = [\text{HS}(\text{CH}_2)_{11}\text{CH}_3]_{\text{sol}}/[\text{HS}(\text{CH}_2)_{21}\text{CH}_3]_{\text{sol}}$ in the range 1 to 100, together with monolayers of the two pure thiols. Both pure monolayers were autophobic and oleophobic: $\theta_a(\text{HD}) = 47^\circ$ for $\text{HS}(\text{CH}_2)_{21}\text{CH}_3$, $\theta_a(\text{HD}) = 46^\circ$ for $\text{HS}(\text{CH}_2)_{11}\text{CH}_3$. The contact angles on the mixed monolayers were lower than on the pure monolayers and reached a minimum between $R = 10$ and $R = 30$. There was a strong preference for adsorption of the longer thiol. The minimum in the contact angle of hexadecane occurred at an ellipsometric thickness intermediate between the thicknesses of the two pure monolayers, but the change in thickness with increasing R was too rapid to establish from these data the composition of the monolayer that would yield the most oleophilic surface. The form of the plot of contact angles against R is consistent with our hypothesis that the two components in the monolayer do not phase-segregate into macroscopic islands (Figure 1); if they did, each of the islands would be oleophobic, and we would expect $\theta_a(\text{HD})$ to be independent of the composition of the monolayer. The contact angles in Fig. 3 were measured after the gold slides had been immersed in the adsorption solutions for six days. The contact angles were unchanged after the slides had been reimmersed in the adsorption solutions for an additional three weeks.

$\text{HS}(\text{CH}_2)_{21}\text{CH}_3 + \text{HS}(\text{CH}_2)_{11}\text{CH}_3$ Adsorbed from Isooctane. If the

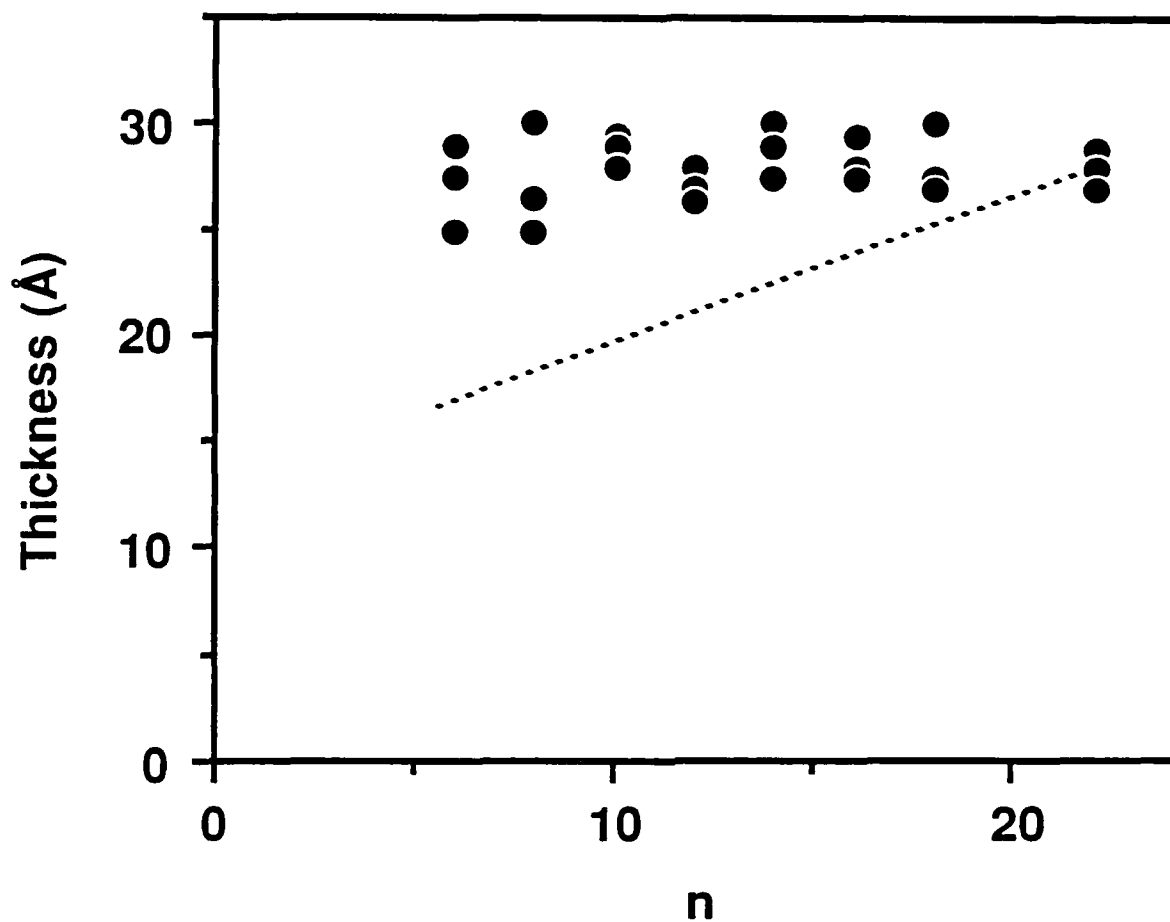


Figure 2. Ellipsometric thicknesses of monolayers adsorbed onto gold from 1 mM solutions in ethanol containing a 1:1 mixture of $\text{HS}(\text{CH}_2)_{21}\text{CH}_3$ and $\text{HS}(\text{CH}_2)_{n-1}\text{CH}_3$. The dotted line represents the thickness expected if the composition of the monolayer and the solution were the same.

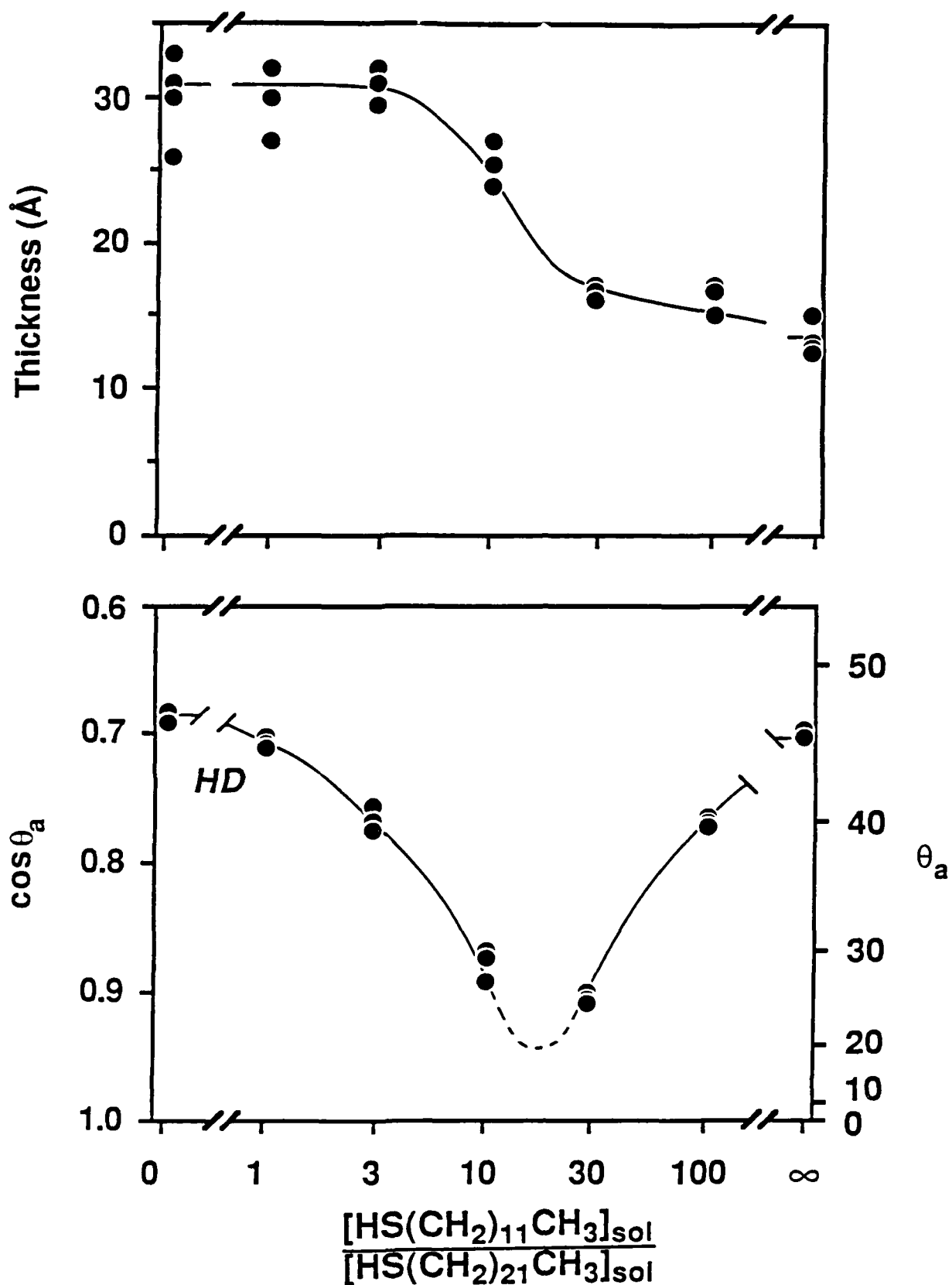
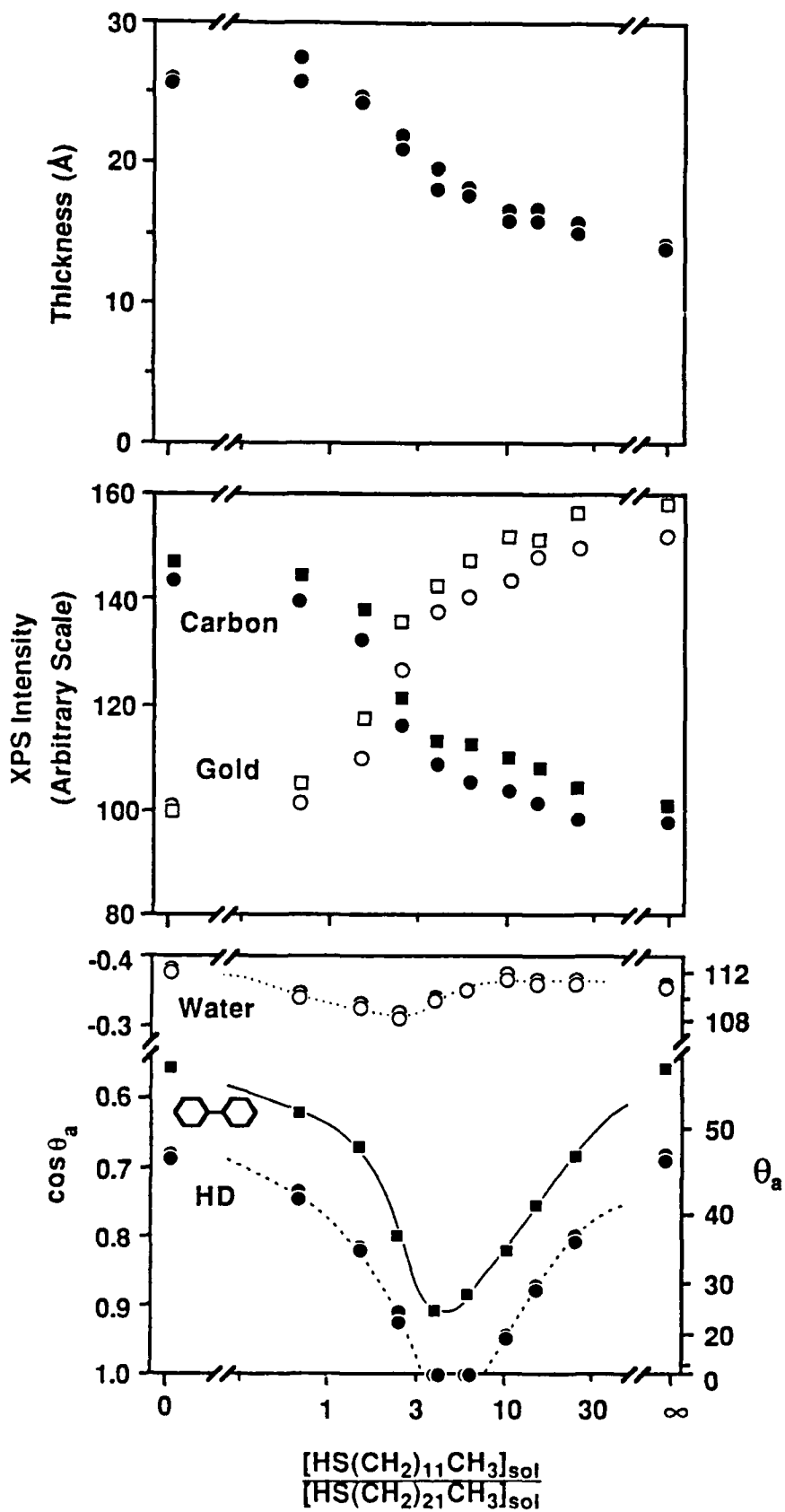


Figure 3. Monolayers adsorbed onto gold from ethanolic solutions containing mixtures of $\text{HS}(\text{CH}_2)_{21}\text{CH}_3$ and $\text{HS}(\text{CH}_2)_{11}\text{CH}_3$: ellipsometric thickness (upper figure) and advancing contact angle of hexadecane (lower figure) are plotted against the ratio of $\text{HS}(\text{CH}_2)_{11}\text{CH}_3$ to $\text{HS}(\text{CH}_2)_{21}\text{CH}_3$ in solution. The line in the lower figure has been added as an aid to the eye; we cannot determine from these data alone the depth of the minimum in $\theta_a(\text{HD})$.

preference for adsorption of the longer chain from ethanol is thermodynamic, the composition of the monolayer should be influenced by the relative chemical potentials of the two components in solution. Intuitively, we would expect a smaller difference between the chemical potentials of a long- and a short-chained thiol in a hydrocarbon solvent than in an alcohol. As a consequence, we might expect to observe a smaller preference for adsorption of the long chain from isooctane than from ethanol. Mixtures of $\text{HS}(\text{CH}_2)_{21}\text{CH}_3$ and $\text{HS}(\text{CH}_2)_{11}\text{CH}_3$ were adsorbed onto gold from isooctane. The values of R were clustered more closely around the minimum in θ than was the case in Fig. 3 (a preliminary experiment was performed to locate the approximate position of the minimum in θ). Figure 4 shows the ellipsometric thicknesses of the monolayers, the intensities of the $\text{C}(1s)$ and $\text{Au}(4f_{7/2})$ photoelectron peaks in XPS, the advancing contact angles of water and hexadecane (measured after immersion of the gold slides in the adsorption solutions for one day), and the advancing contact angle of bicyclohexyl (measured after immersion for ten days). We observed no significant change in the advancing contact angles of water and hexadecane between one day's and ten days' immersion. As we predicted on the basis of thermodynamics, the midpoint in the ellipsometric thickness and in the XPS intensities -- an approximate gauge of the midpoint in the composition of the monolayer -- and the minimum in the contact angle of hexadecane moved to lower values of R , compared to the adsorptions performed in ethanol. We also note the unexpected observation that the minima in the advancing contact angles of water and hexadecane occurred at different values of R , and that the minimum in the contact angle of hexadecane did not coincide with the maximally mixed monolayer (i.e. the monolayer containing equal amounts of the two components).

The minimum in the contact angle of hexadecane on the monolayers adsorbed from isooctane appeared to be deeper than on the monolayers adsorbed from ethanol (Figs. 3, 4 and 7). From isooctane, wettable monolayers were formed over a range of R , from ethanol the minimum values of $\theta_a(\text{HD})$ were 25° and 18° in two repetitions of the experiment.

Figure 4. Monolayers adsorbed onto gold from mixed solutions of HS(CH₂)₂₁CH₃ and HS(CH₂)₁₁CH₃ in isooctane. The abscissa represents the ratio of concentrations in solution on a logarithmic scale. Upper figure: ellipsometric thickness. Middle figure: intensity of the C(1s) (solid symbols) and Au(4f_{7/2}) photoelectron peaks (open symbols) in XPS. The areas of the gold peaks have been rescaled for clarity of presentation. The squares and circles represent two separate series of samples. The samples within each series were loaded into the spectrometer simultaneously and run sequentially. Lower figure: advancing contact angles of water (open circles), bicyclohexyl (squares) and hexadecane (solid circles). The lines have been added as aids to the eye and have no theoretical significance.



There are two possible explanations for this difference. First, wettable monolayers can also be formed from ethanol, but no data points were taken at appropriate values of R . Figure 7, in particular, suggests that this possibility is unlikely: if wettable monolayers can be adsorbed from ethanol, the dip in the contact angle of hexadecane would have to be much sharper when ethanol is the solvent than when the adsorptions are performed from isooctane. Alternatively, the mixed monolayers adsorbed from isooctane were indeed more oleophilic than monolayers of the same composition adsorbed from ethanol, possibly because the outer part of the monolayer was more disordered and liquid-like. In either case, the nature of the solvent has an effect on the structure of the monolayer, in addition to shifting the position of the equilibrium between monolayer and solution.

We estimated the composition of the mixed monolayers by comparing the ratio of the intensities of the $C(1s)$ and $Au(4f_{7/2})$ photoelectrons, obtained by XPS, with the ratios from monolayers of pure $HS(CH_2)_{n-1}CH_3$ (adsorbed from ethanol). Figure 5 shows the C/Au ratios calculated from the data in Fig. 4, together with the equivalent chain lengths, n , of pure monolayers of alkanethiols. We estimated the composition of the monolayers by assuming that χ^{C12} , the mole fraction of dodecanethiol in the monolayer, was linearly related to the equivalent chain length. We used the data from XPS rather than from ellipsometry to calculate the compositions because the data from XPS contained less scatter and yielded more precise compositions.²⁸ Figure 6 plots the advancing contact angles of water and hexadecane against χ^{C12} for mixed monolayers of $HS(CH_2)_{11}CH_3$ and $HS(CH_2)_{21}CH_3$ adsorbed from isooctane. The contact angle of water had a broad, shallow minimum near $\chi^{C12} = 0.5$, whereas the contact angle of hexadecane reached a minimum around $\chi^{C12} = 0.8$ (that is, $[CH_3(CH_2)_{11}S^-]_{surf}/[CH_3(CH_2)_{21}S^-]_{surf} = 4$). The scatter in the data gives an indication of random errors.

Contact Angles of Dispersive Liquids on Mixed Monolayers of $HS(CH_2)_{11}CH_3$ and $HS(CH_2)_nCH_3$ Adsorbed from Ethanol. Theories of wetting, such as Fowkes's application of the geometric mean approximation (see below), predict

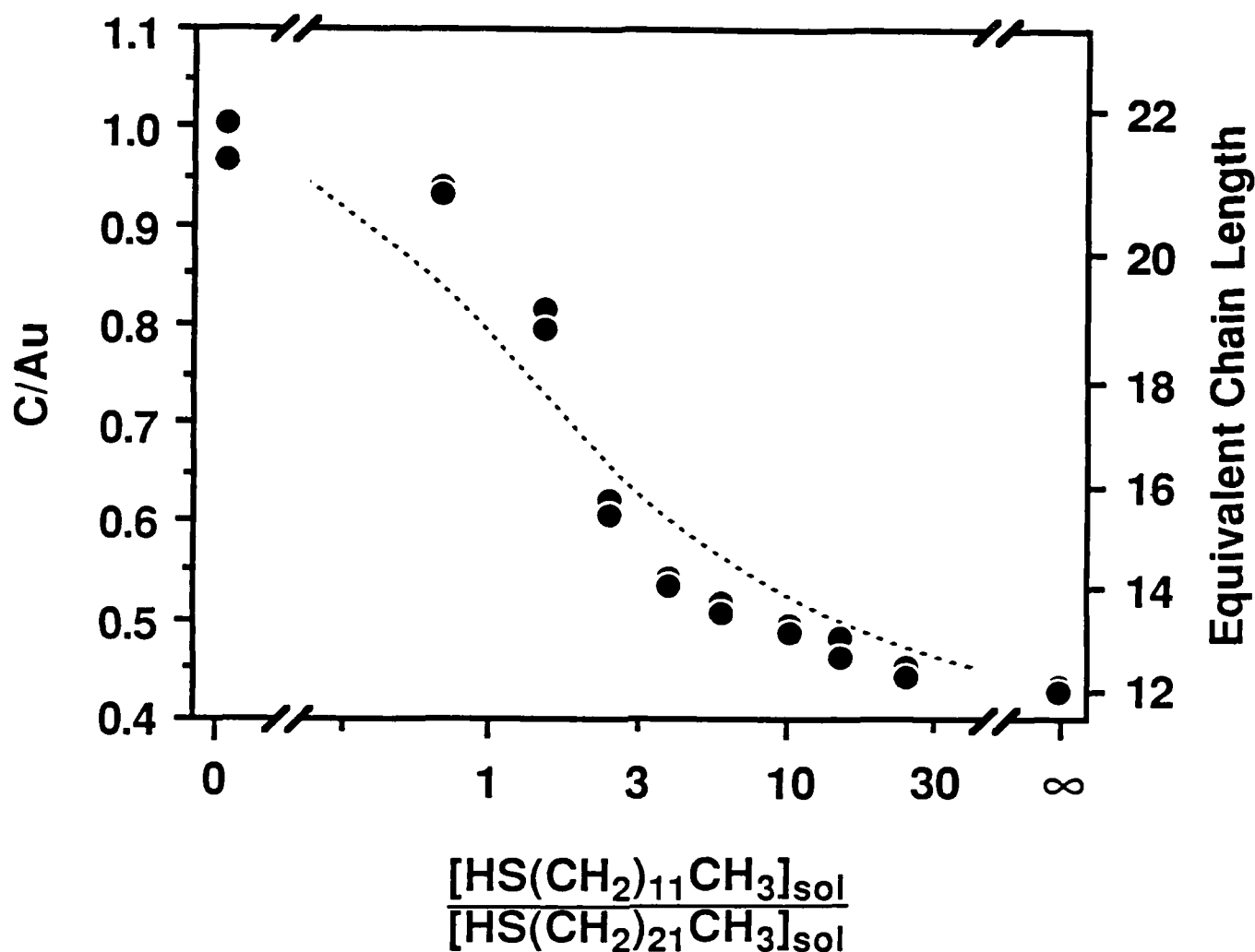


Figure 5. Ratio of C(1s) to Au(4f_{7/2}) peak areas in XPS for monolayers adsorbed onto gold from solutions of HS(CH₂)₂₁CH₃ and HS(CH₂)₁₁CH₃ in isooctane. The right-hand axis shows the equivalent chain length, *n*, of a pure monolayer of HS(CH₂)_{*n*-1}CH₃, adsorbed from ethanol, that yields the same ratio of C/Au. The scatter in the data gives an indication of the random errors. The dotted line represents the ratio of C/Au peak areas expected theoretically if $[C_{22}]_{\text{surf}}[C_{12}]_{\text{sol}}/[C_{12}]_{\text{surf}}[C_{22}]_{\text{sol}} = 2.3$.

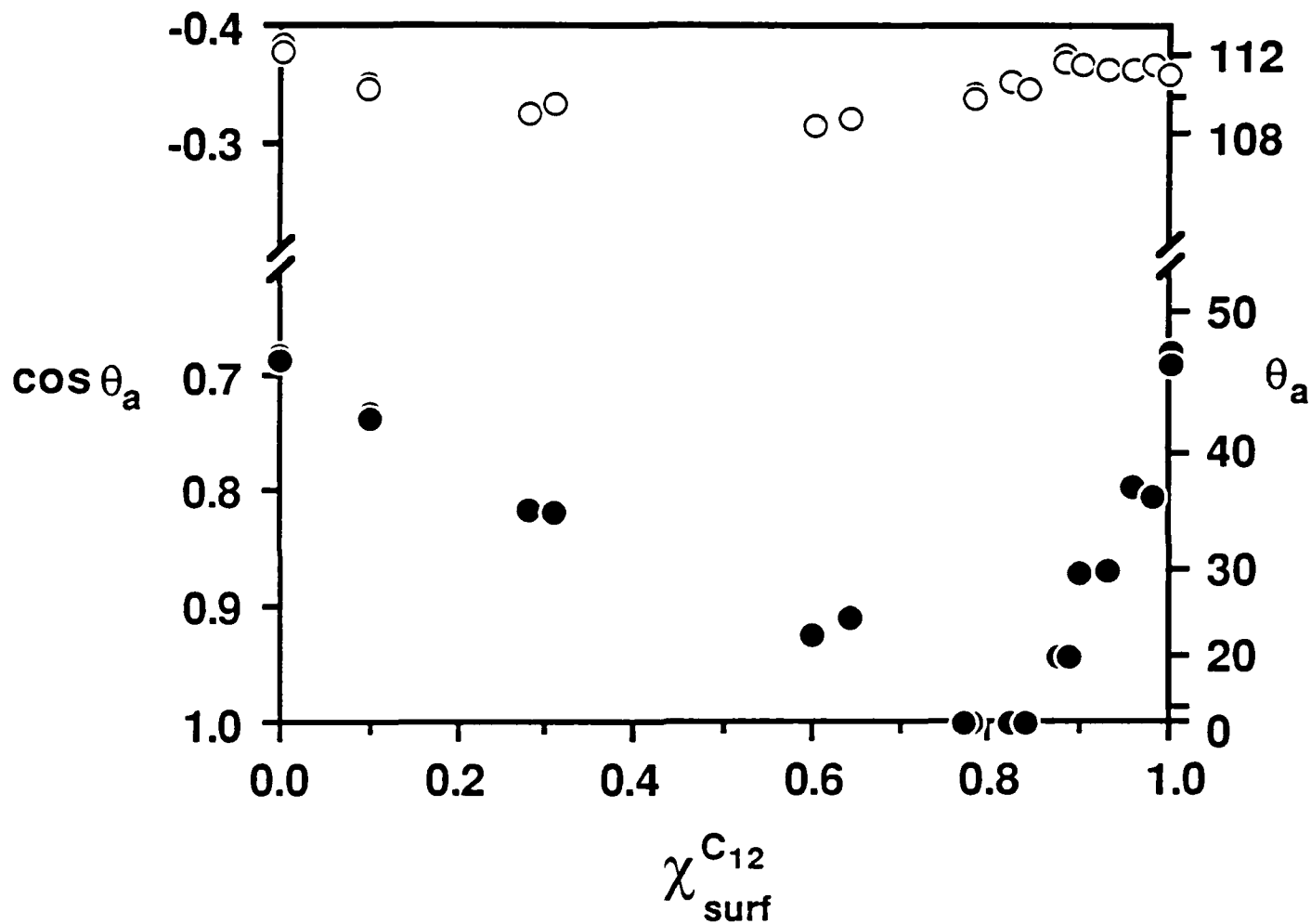


Figure 6. Advancing contact angles of water (open circles) and hexadecane (solid circles) plotted against the mole fraction of HS(CH₂)₁₁CH₃ in a monolayer adsorbed from mixtures of HS(CH₂)₂₁CH₃ and HS(CH₂)₁₁CH₃ in isooctane. The mole fraction of HS(CH₂)₁₁CH₃ in the monolayer was calculated from the XPS data shown in Figure 5. The errors in the contact angles are within the symbols.

how the contact angles of liquids on dispersive surfaces should vary with the surface tension of the liquid.⁹ To test these theories we measured the contact angles of four dispersive liquids (decane, hexadecane, bicyclohexyl, and α -bromonaphthalene) on mixed monolayers of $\text{HS}(\text{CH}_2)_{11}\text{CH}_3$ and $\text{HS}(\text{CH}_2)_{21}\text{CH}_3$ adsorbed from ethanol (Figure 7).²⁹ We chose decane as one of these liquids because its size matches the difference in chain lengths between the two adsorbates.³⁰ Bicyclohexyl and α -bromonaphthalene are liquids with high surface tensions that would be unable to penetrate into the cylindrical holes left by a molecule of dodecanethiol ($\text{HS}(\text{CH}_2)_{11}\text{CH}_3$) in a monolayer composed predominantly of docosanethiol ($\text{HS}(\text{CH}_2)_{21}\text{CH}_3$). These last two liquids did not wet any of the mixed methyl-terminated monolayers and hence gave information on interfacial free energies over the complete range of R .

If the difference between the lengths of the chains of the two thiols were smaller, we would expect intuitively that the minimum in θ would move to lower values of R and the changes in the contact angles would become less pronounced. Figure 8 shows the ellipsometric thickness and advancing contact angles on monolayers adsorbed from mixtures of $\text{HS}(\text{CH}_2)_{15}\text{CH}_3$ and $\text{HS}(\text{CH}_2)_{11}\text{CH}_3$ in ethanol, a difference of four carbons in the length of the chain. The minimum in θ occurs near $R = 5$, compared to $R = 15\text{--}30$ for $\text{HS}(\text{CH}_2)_{21}\text{CH}_3/\text{HS}(\text{CH}_2)_{11}\text{CH}_3$, and the changes in the contact angles were smaller than in the mixed monolayers with a difference of ten carbons in the chain length.

Hysteresis on Mixed Methyl/Methylene Surfaces. We expect the disorder in the outer part of the mixed monolayers to expose both the terminal methyl groups and the polymethylene chains at the surface. We are interested in the effect of such microscopic heterogeneity on the hysteresis in the contact angle. Figure 9 plots the hysteresis in the contact angle on the mixed monolayers of $\text{HS}(\text{CH}_2)_n\text{CH}_3$ and $\text{HS}(\text{CH}_2)_{11}\text{CH}_3$ adsorbed from ethanol and isooctane. Data were not included in these graphs if the receding contact angle was zero. The hysteresis in the contact angles of hydrocarbons on monolayers adsorbed from ethanol was essentially independent of the composition of the monolayers,

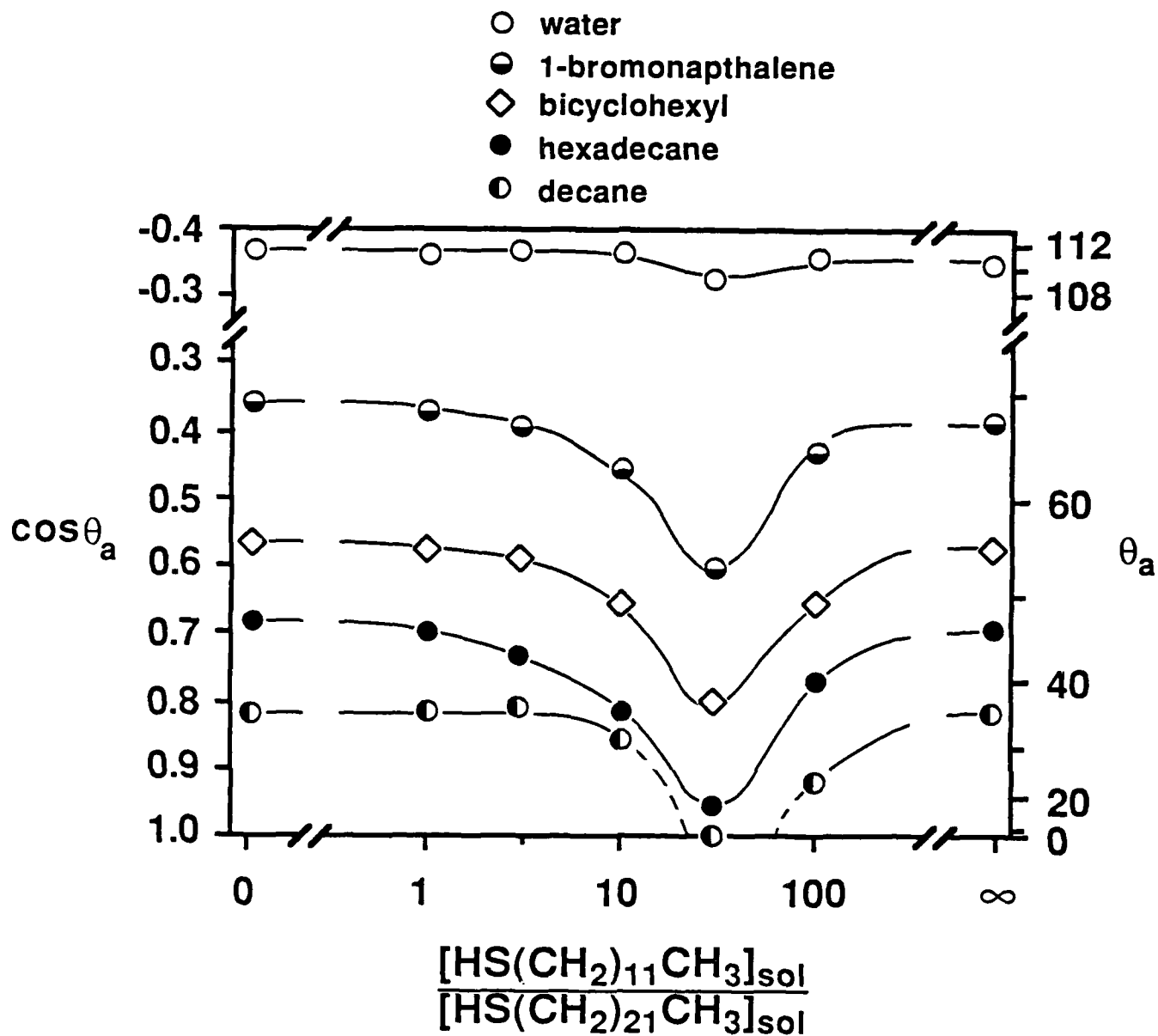


Figure 7. Advancing contact angles of water (○), α -bromonaphthalene (◐), bicyclohexyl (◇), hexadecane (●) and decane (◑) on mixed monolayers of $\text{HS}(\text{CH}_2)_{21}\text{CH}_3$ and $\text{HS}(\text{CH}_2)_{11}\text{CH}_3$ adsorbed onto gold from ethanol. The lines are provided only as an aid to the eye.

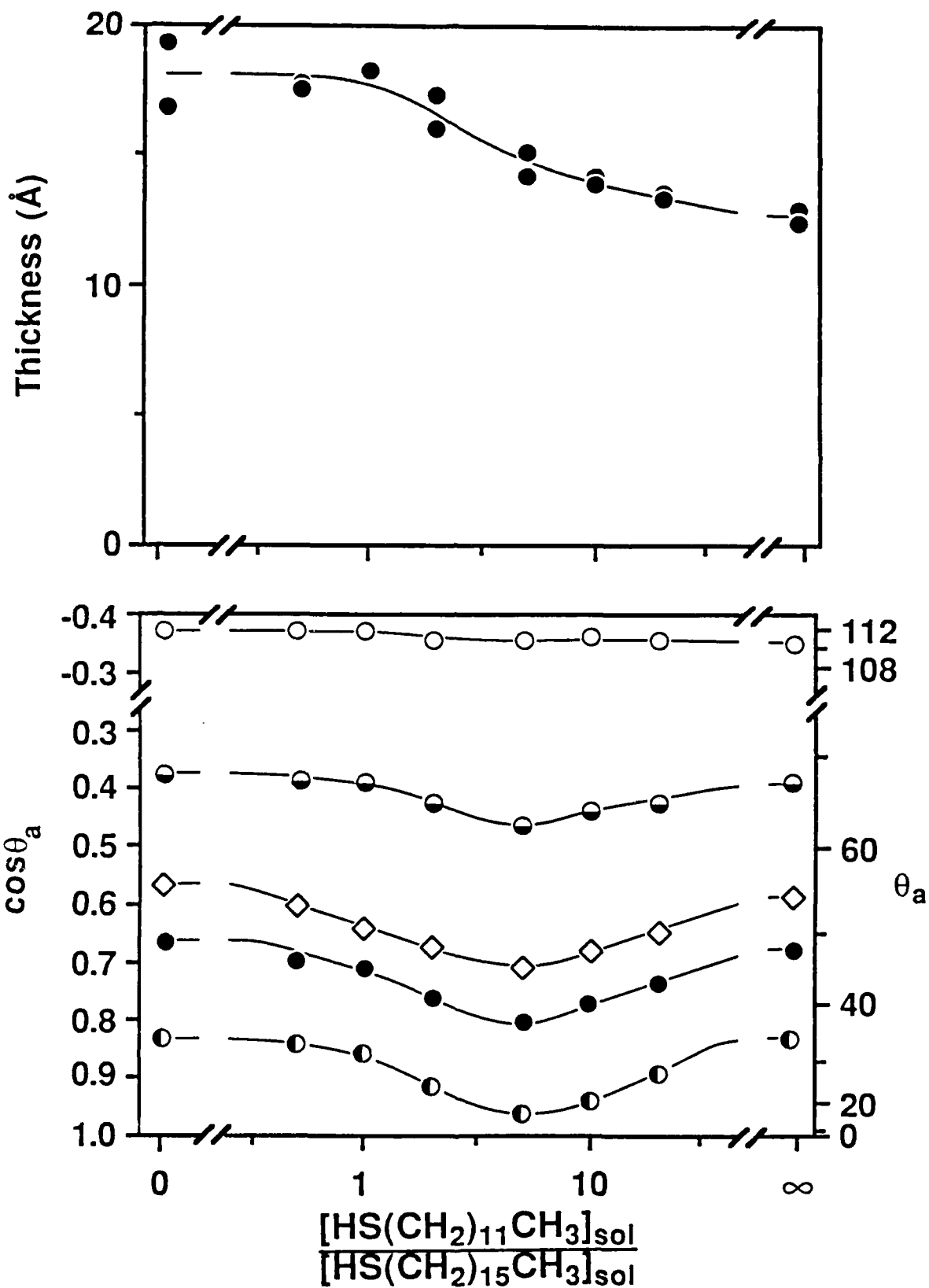
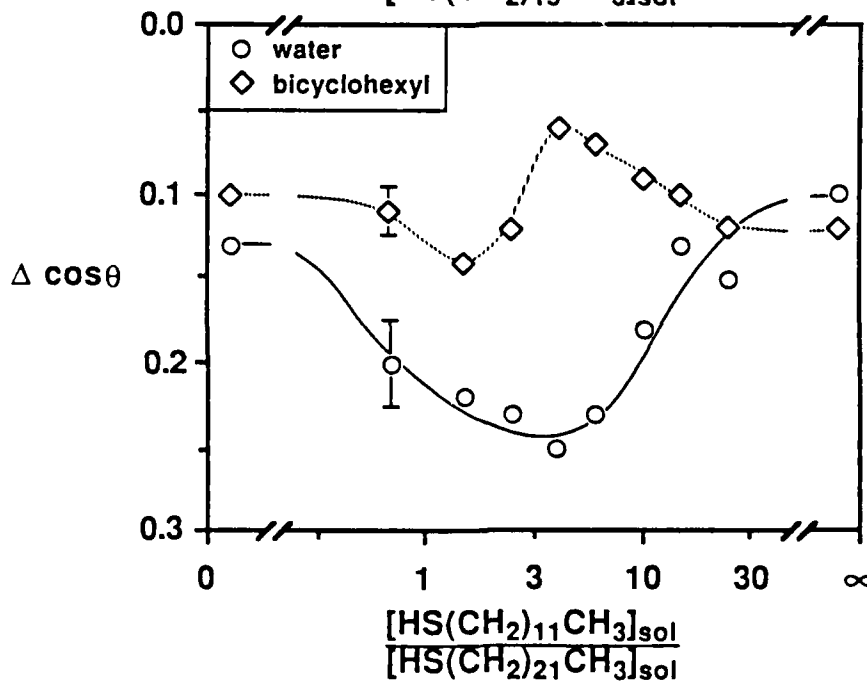
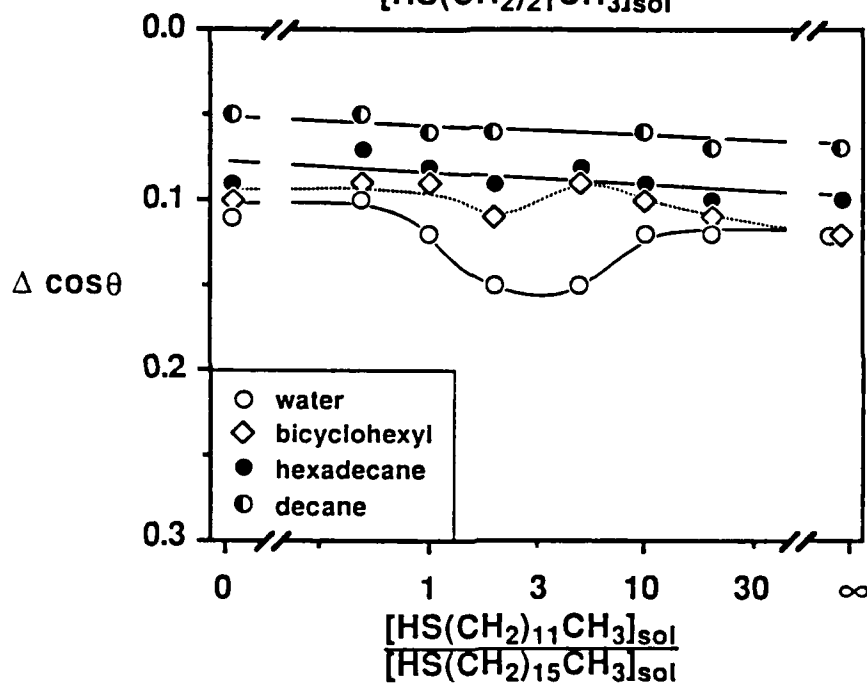
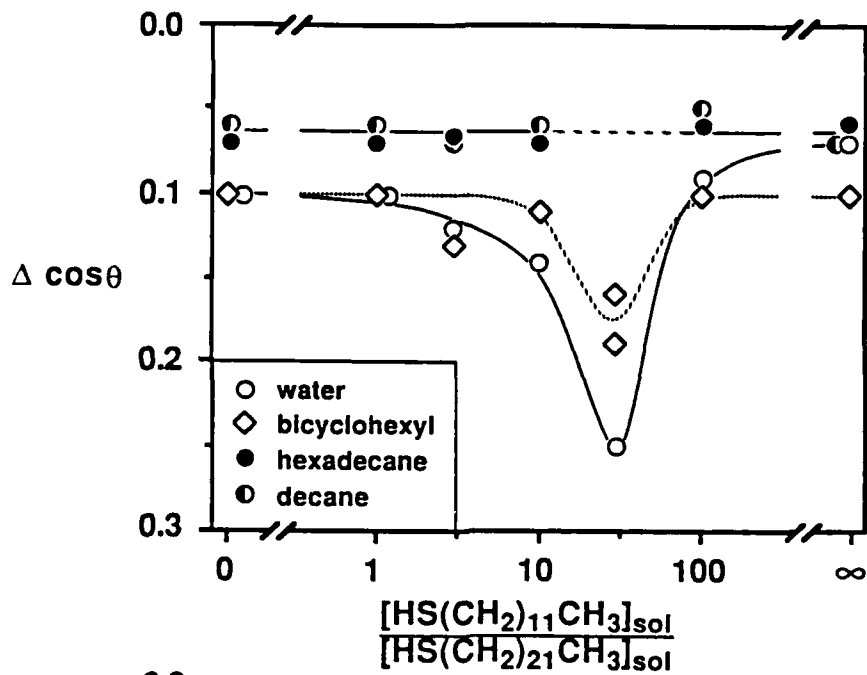


Figure 8. Ellipsometric thickness (upper figure) and advancing contact angles (lower figure) of mixed monolayers of $\text{HS}(\text{CH}_2)_{15}\text{CH}_3$ and $\text{HS}(\text{CH}_2)_{11}\text{CH}_3$ adsorbed onto gold from ethanol: water (○), α -bromonaphthalene (●), bicyclohexyl (◊), hexadecane (●) and decane (○).

Figure 9. Hysteresis in the contact angles on mixed methyl-terminated monolayers on gold. Upper Figure: $\text{HS}(\text{CH}_2)_{21}\text{CH}_3$ and $\text{HS}(\text{CH}_2)_{11}\text{CH}_3$ adsorbed from ethanol. Middle Figure: $\text{HS}(\text{CH}_2)_{15}\text{CH}_3$ and $\text{HS}(\text{CH}_2)_{11}\text{CH}_3$ adsorbed from ethanol. Lower Figure: $\text{HS}(\text{CH}_2)_{21}\text{CH}_3$ and $\text{HS}(\text{CH}_2)_{11}\text{CH}_3$ adsorbed from isooctane. $\Delta \cos \theta = \cos$ ine of the minimum receding contact angle minus cosine of the advancing contact angle. Lines have been added to these graphs purely as aids to the eye. The variation in the hysteresis in the contact angle of bicyclohexyl in the middle figure may be significant, or may simply arise from random errors. Estimated limits of error are shown in the lower figure.



with the exception of bicyclohexyl on the monolayer adsorbed at $R = 30$. On monolayers adsorbed from isooctane, the variations in the hysteresis in the contact angle of bicyclohexyl did not correlate with the changes in the advancing or the receding contact angle.

α -Bromonaphthalene appeared slowly to cause damage to the thinner monolayers. As a result, the hysteresis in the contact angle increased gradually from 0.16 on the monolayer of $\text{HS}(\text{CH}_2)_{21}\text{CH}_3$ to 0.21 on the monolayer of $\text{HS}(\text{CH}_2)_{11}\text{CH}_3$. The hysteresis in the contact angle was not correlated with the contact angle itself: no increase in hysteresis was observed on the monolayers near the minimum in the contact angle.

The advancing contact angle of water was very insensitive to the composition of the monolayer, but the hysteresis in the contact angle of water was greater on the mixed monolayers than on the pure monolayers for all the methyl-terminated systems studied.

$\text{HS}(\text{CH}_2)_{11}\text{OH} + \text{HS}(\text{CH}_2)_{19}\text{OH}$ Adsorbed from Ethanol. In monolayers comprising mixtures of methyl-terminated thiols of different chain lengths, the disordered outer phase caused a decrease in the contact angle of hexadecane. Pure monolayers of $\text{HS}(\text{CH}_2)_{11}\text{OH}$ or $\text{HS}(\text{CH}_2)_{19}\text{OH}$ show wetting or near wetting behavior with water ($\theta_a(\text{H}_2\text{O}) < 10^\circ$ and $< 15^\circ$, respectively). In monolayers comprising mixtures of these two thiols, disorder in the outer part of the monolayer should expose nonpolar methyl groups at the surface and cause an increase in the contact angle of water. Figure 10 plots the ellipsometric thickness and the advancing contact angle of water for mixed monolayers of $\text{HS}(\text{CH}_2)_{11}\text{OH}$ and $\text{HS}(\text{CH}_2)_{19}\text{OH}$.⁶ The contact angle showed a pronounced maximum supporting our model of a disordered outer phase in the monolayer, and militating against the formation of macroscopic, single-component domains. Figure 11 plots the contact angles of water against the composition of the monolayer, calculated on the assumption that the ellipsometric thickness (Fig. 10) was a linear function of the mole fraction of the shorter thiol in the monolayer, $\chi_{\text{surf}}^{\text{C11}}$. The standard errors shown were estimated from the distribution of the differences between the measured thicknesses of the

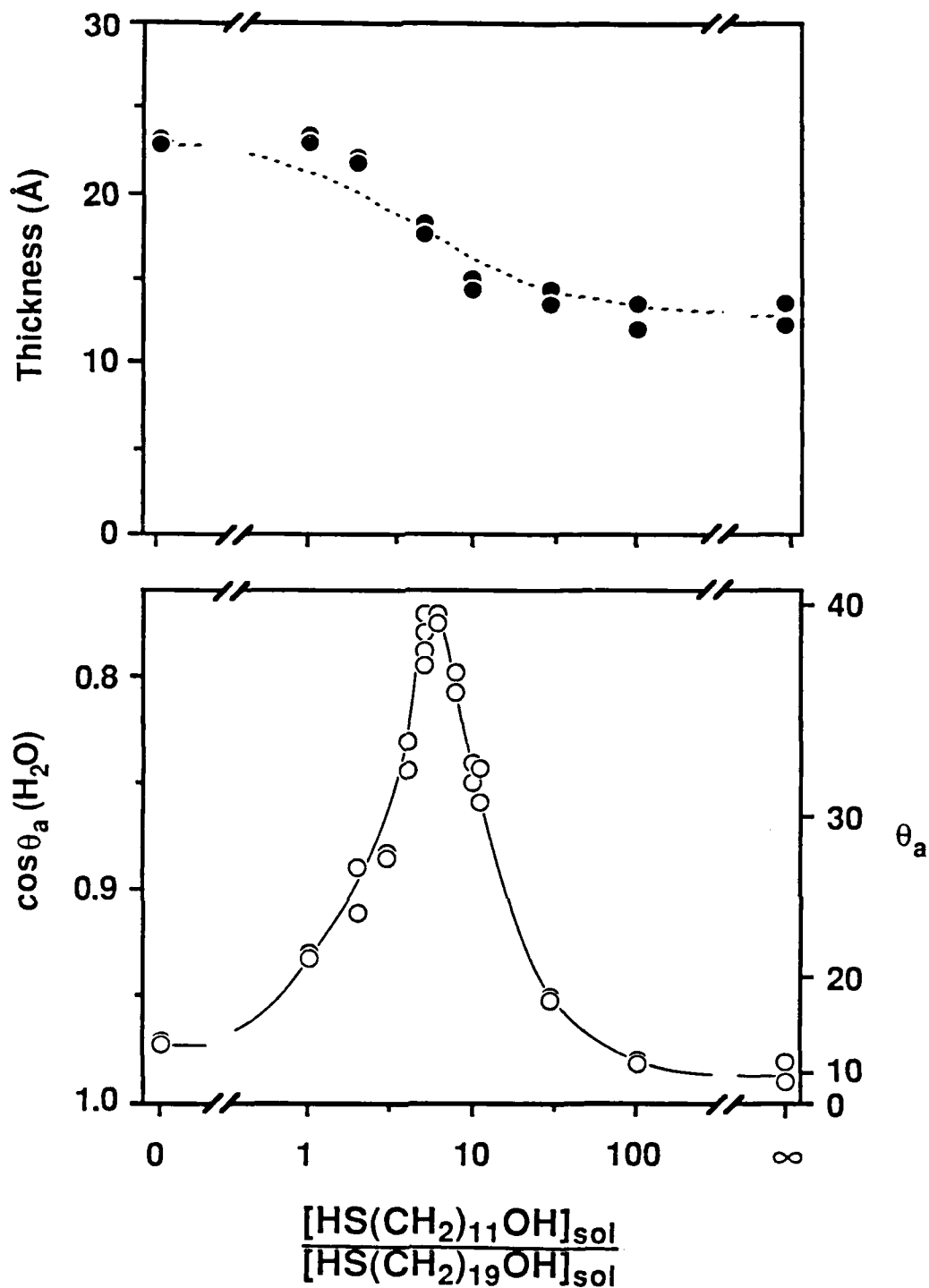


Figure 10. Mixed monolayers of $\text{HS}(\text{CH}_2)_{11}\text{OH}$ and $\text{HS}(\text{CH}_2)_{19}\text{OH}$ adsorbed onto gold from ethanol: ellipsometric thickness (upper figure) and advancing contact angles of water (lower figure) as a function of the concentrations in solution. The lower figure includes additional data, in the region of the peak maximum, that are not shown in the upper figure. The dotted line in the upper figure represents the thickness expected theoretically if $[\text{C}_{19}]_{\text{surf}}[\text{C}_{11}]_{\text{sol}}/[\text{C}_{11}]_{\text{surf}}[\text{C}_{19}]_{\text{sol}} = 5$. The solid line in the lower figure is included as an aid to the eye.

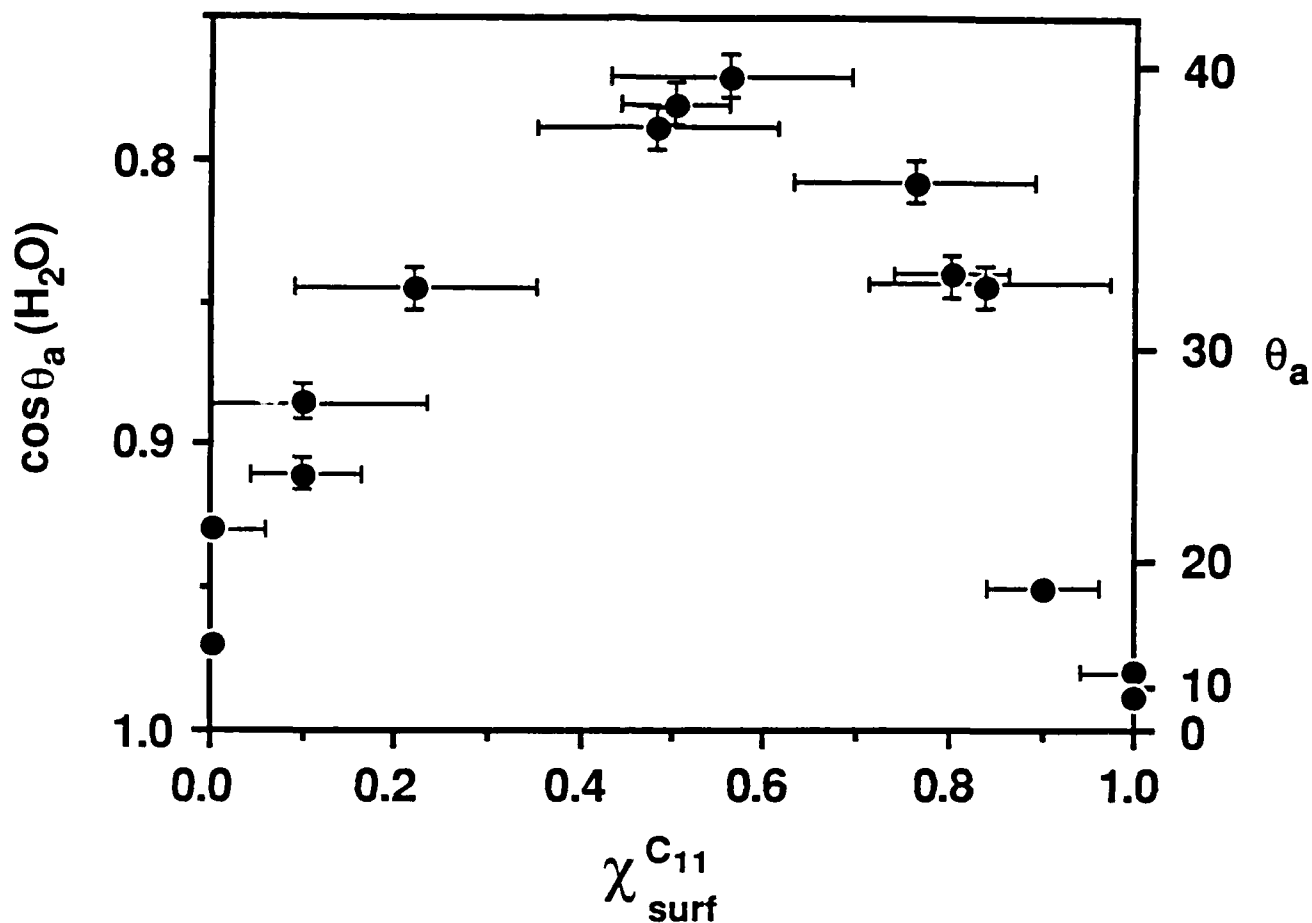


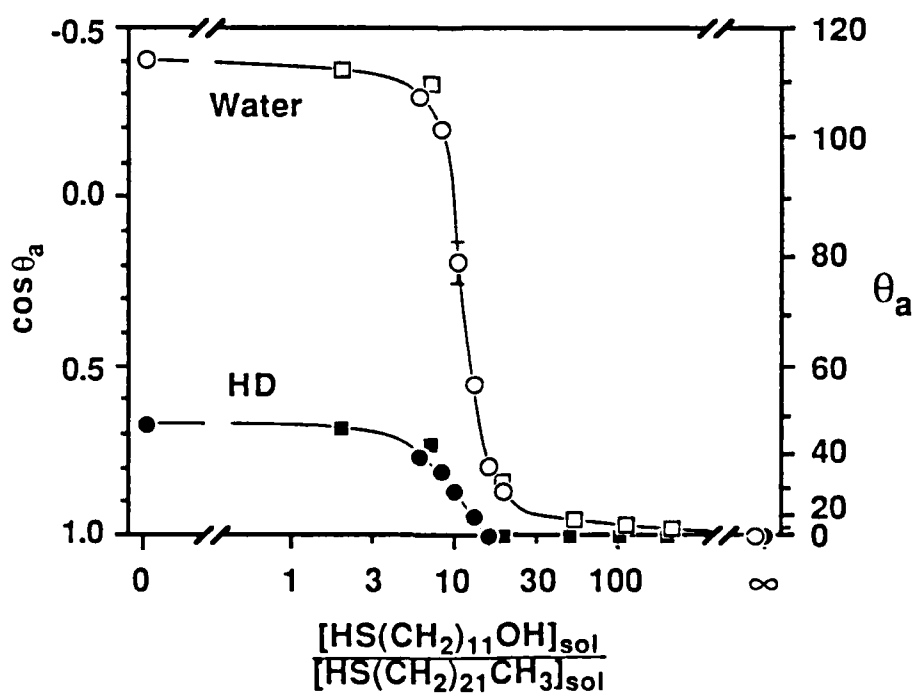
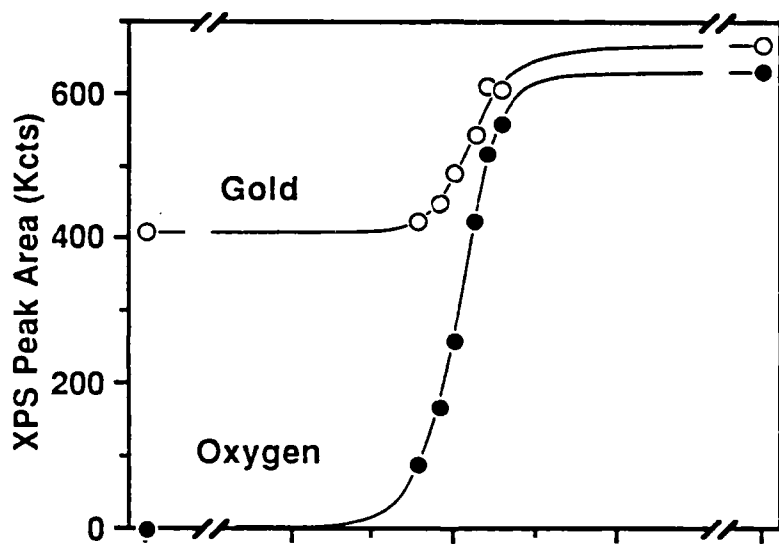
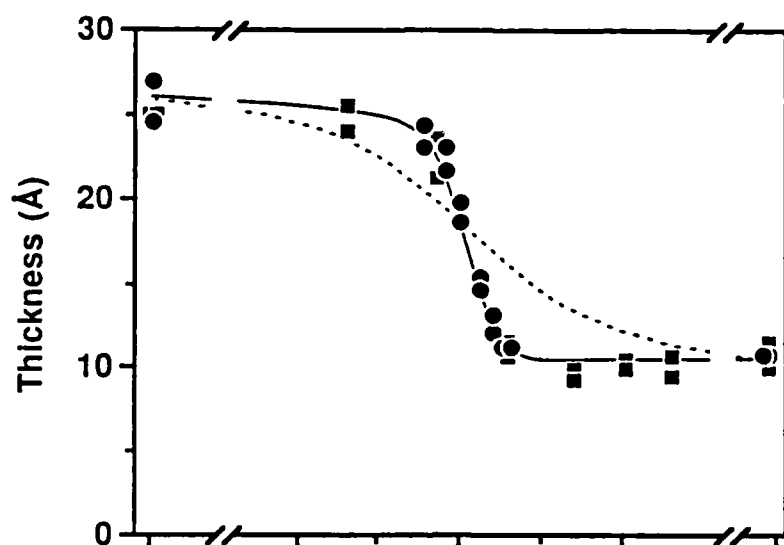
Figure 11. Advancing contact angles of water on mixed monolayers of $\text{HS}(\text{CH}_2)_{11}\text{OH}$ and $\text{HS}(\text{CH}_2)_{19}\text{OH}$ on gold, plotted against the mole fraction of $\text{HS}(\text{CH}_2)_{11}\text{OH}$ in the monolayer. The composition of the monolayer was calculated from the ellipsometric thicknesses. The standard error bars were estimated from the differences in ellipsometric thickness between the monolayers on pairs of gold slides immersed in the same solutions.

monolayers on the two slides in each solution. The maximum in θ occurred at $\chi_{\text{surf}}^{\text{C11}} = 0.5-0.6$. At the time these measurements were made, the monolayers had not fully reached equilibrium. Over a period of several weeks the maximum in the contact angle increased from $R = 6$ to $R \approx 11$.

HS(CH₂)₁₁OH + HS(CH₂)₂₁CH₃ Adsorbed from Ethanol. Although we are confident that macroscopic islands ($\geq 0.1 \mu\text{m}$, *vide infra*) do not form in the monolayers, the degree to which small aggregates or clusters of molecules of one species occur is unclear. To approach this problem we synthesized mixed monolayers of a short, hydroxyl-terminated thiol and a longer methyl-terminated thiol. The degree to which the polar hydroxyl group in these mixed monolayers is sensed by a contacting liquid may be a sensitive function of the distribution of the two components on a molecular length scale.

Figure 12 plots the ellipsometric thickness, XPS intensities, and advancing contact angles of water and hexadecane, measured after overnight immersion, against the ratio of the two components in solution. All the experimental quantities measured showed a dramatic change over a narrow range in composition, $R = 7-20$. As with the monolayers comprising two hydroxyl-terminated thiols (above), these monolayers had not reached their limiting composition when the measurements were made. Figure 13 shows contact angles measured after reimmersion of the gold slides in the adsorption solutions for an additional nine days. The advancing contact angles of water (filled circles) suggest that the midpoint in the composition had moved from $R = 11$ to $R \approx 14$ over the previous nine days. The values of $\theta_a(\text{H}_2\text{O})$ measured after overnight immersion are shown by the solid line. The solid bars indicate the values of the maximum advancing³¹ and the minimum receding contact angles of water. We observed large hysteresis in the contact angles on the mixed monolayers. Figure 13 also shows the advancing contact angles of glycerol on the monolayers formed after ten days' immersion. Glycerol is a highly polar molecule but is bulkier and hence more sterically hindered than water. The contact angles of glycerol suggest that glycerol may be less able than water to penetrate into the monolayer to form

Figure 12. Competitive adsorption of HS(CH₂)₁₁OH and HS(CH₂)₂₁CH₃ from solution in ethanol onto gold. Squares and circles represent two separate experiments. Upper figure: ellipsometric thickness. The dotted line represents the thickness expected theoretically, using the experimental thicknesses for the pure monolayers, if $[C_{22}]_{\text{surf}}[C_{11}]_{\text{sol}}/[C_{11}]_{\text{surf}}[C_{22}]_{\text{sol}} = 11$. Middle figure: areas of the O(1s) and Au(4f_{7/2}) peaks in the XPS spectra. Lower figure: advancing contact angles of water and hexadecane. Each symbol represents two data points. With one exception, the variation in contact angle lay within the size of the symbol on the graph: an error bar is shown to indicate the difference in contact angles for the single exception.



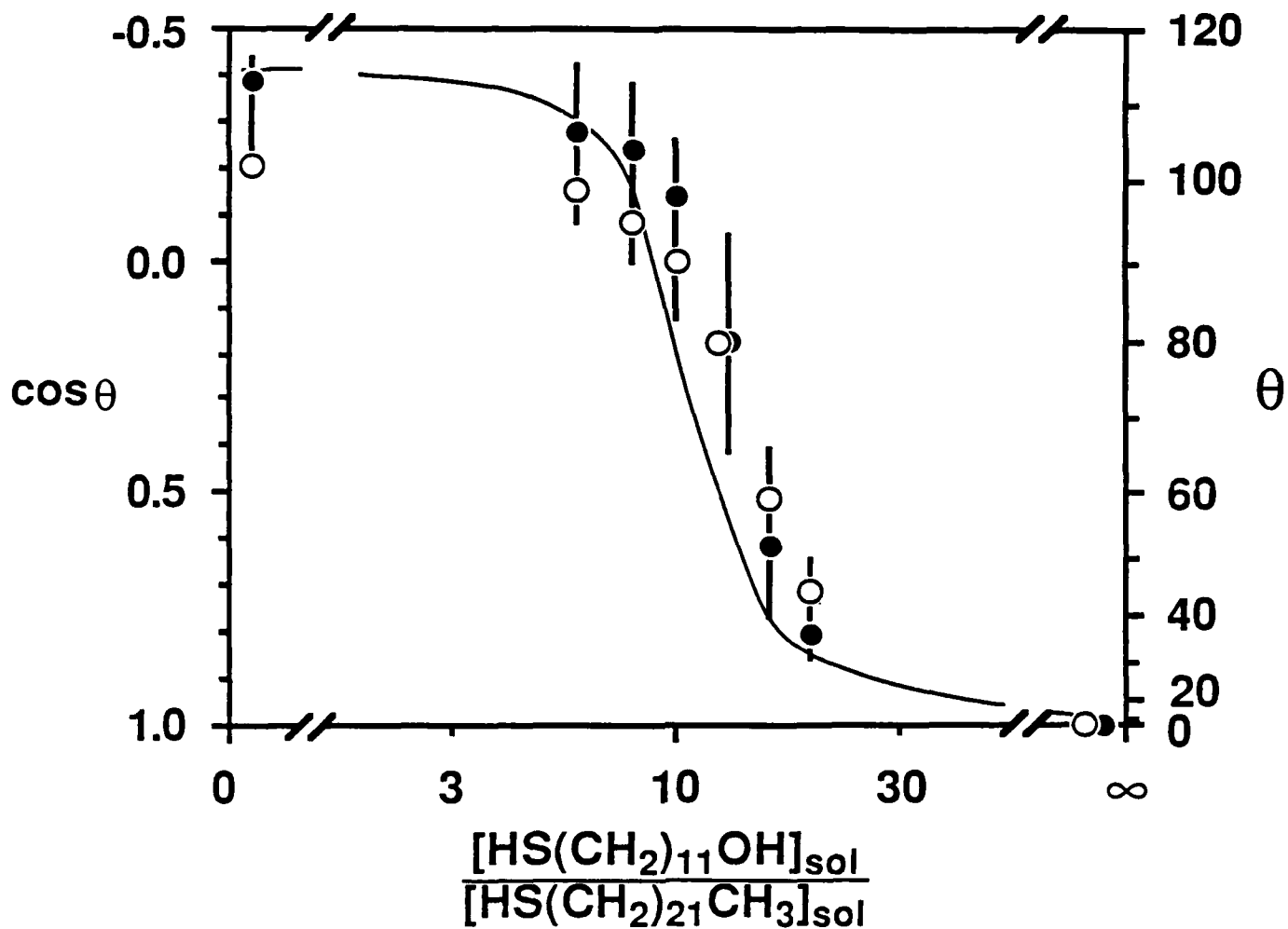


Figure 13. Contact angles on mixed monolayers of $HS(CH_2)_{11}OH$ and $HS(CH_2)_{21}CH_3$ measured after immersion of the gold slides in the adsorption solutions for ten days. The filled circles represent the advancing contact angles of water measured by forming a drop at the end of a needle, lowering the drop to the surface, and removing the needle. The solid line shows the values of the advancing contact angle of water on the same slides after they had only been immersed in the adsorption solutions overnight (from Fig. 12). The solid bars indicate the values of the maximum advancing and minimum receding contact angles of water, measured by the technique of Dettre and Johnson.⁵⁷ The open circles represent the advancing contact angles of glycerol, also measured after 10 days. Glycerol was used to probe the accessibility of the hydroxyl groups to an H-bonding liquid that is more sterically hindered than water. The drops of glycerol were left for several minutes on the surface before the contact angles were measured to ensure that the limiting contact angles had been reached.

hydrogen bonds to hydroxyl groups that are buried within a monolayer composed largely of docosanethiol moieties.

Discussion

The relationship between the composition of the monolayer and the composition of the solution can be rationalized in terms of the relative solubilities of the two components and the excess free energies of mixing in the solution and in the monolayer. In all the systems studied, adsorption of the longer chain was preferred over the shorter chain. The value of R that resulted in a 1:1 mixture of the two components in the monolayer varied from system to system, and between solvents: R = 2.3 for HS(CH₂)₂₁CH₃/HS(CH₂)₁₁CH₃ from isooctane; R = 3 for HS(CH₂)₁₅CH₃/HS(CH₂)₁₁CH₃ from ethanol; R = 5 for HS(CH₂)₁₉OH/HS(CH₂)₁₁OH from ethanol; R = 11 for HS(CH₂)₂₁CH₃/HS(CH₂)₁₁OH from ethanol; and R = 15 for HS(CH₂)₂₁CH₃/HS(CH₂)₁₁CH₃ from ethanol. The monolayers containing only methyl-terminated components did not exhibit any time-dependence in the contact angles. Those containing hydroxyl-terminated chains had not reached equilibrium when the contact angles were measured. The proportion of the longer chain in these monolayers slowly increased with time.

In the mixed Me/Me monolayers, the preference for adsorption of the longer chain can be understood intuitively on thermodynamic grounds if one recognizes that, to a first approximation, the activity of a thiol in a monolayer is similar to that in a crystal, with a constant additional term to account for the interaction with the gold. The component with the lower solubility, that is the longer chain, will have a higher activity in solution and hence will be preferentially adsorbed into the monolayer. A similar argument holds for mixed monolayers of the two hydroxyl-terminated thiols. Where the tail groups are different, the nature of the solvent influences both the relative solubilities and the relative

activities of the two components in the monolayer: preferential adsorption will vary with the choice of solvent.⁵

The relationship between the concentrations of the two components in the monolayer and in solution was non-ideal. We define a quantity K_{eq} by eq (3)

$$K_{eq} = \frac{[long]_{surf}[short]_{sol}}{[long]_{sol}[short]_{surf}} \quad (3)$$

where [long] and [short] are the concentrations of the longer and the shorter of the two thiols in solution, or thiolates on the surface. In Figures 5, 10, and 12, the dotted line indicates the XPS intensities or ellipsometric thicknesses that would be expected if K_{eq} were a constant given by the value of R for which $[long]_{surf} = [short]_{surf}$. The solutions used in these experiments were sufficiently dilute that we may assume that the activity coefficients in solution were constant. K_{eq} would thus be independent of concentration if the components in the monolayer also behaved ideally. In each case the change in the composition of the monolayer with R was much sharper than would be expected if the monolayer were to act as an ideal two-dimensional solution. By analogy with non-ideal solutions in three dimensions,³² these adsorption isotherms could arise if the excess free energy of mixing of the two components in the monolayer were positive. A positive free energy of mixing would disfavor monolayers containing a mixture of the two components with respect to monolayers composed largely of one component.

The composition of the monolayer and the distribution of the two components within the monolayer are determined by an interplay of enthalpic terms, which favor adsorption of a pure monolayer of one or the other species and self-association of the components within a mixed monolayer, and entropic terms, which drive the formation of mixed monolayers containing two dispersed components. Disruption of the cohesive interactions between pseudo-crystalline hydrocarbon chains in a pure monolayer or the

breaking of hydrogen bonds between hydroxyl groups would both contribute to a positive entropy of mixing. The entropy of mixing can be broken down into three principal components: an ideal combinatorial term of the form $\sum \chi_i \ln \chi_i$, a positive excess term arising from the additional conformations available to the polymethylene chains in a disordered, liquid-like phase compared to the crystalline environment experienced in the pure monolayers, and a negative excess term arising from self-association of the components in the monolayer.

The transition from a monolayer composed predominantly of the long component to one comprising the short component was most abrupt in the mixed monolayers derived from $\text{HS}(\text{CH}_2)_{11}\text{OH}$ and $\text{HS}(\text{CH}_2)_{21}\text{CH}_3$. The energy required to isolate hydroxyl groups in the non-polar environment provided by the alkyl chains of the longer, methyl-terminated thiol would be very large — several kcal/mol of hydroxyl groups. If the hydroxyl-terminated thiols were to form small, internally H-bonded clusters (analogous to those in alkane solvents³³) to reduce the enthalpy of mixing, the entropy of mixing would also be reduced. In solutions of alcohols in alkane solvents, both the enthalpy and the excess free energy of mixing are large and positive.³⁴ Whether the hydroxyl groups are clustered or not, the transition from a pure monolayer of $\text{HS}(\text{CH}_2)_{21}\text{CH}_3$ to a monolayer composed largely of $\text{HS}(\text{CH}_2)_{11}\text{OH}$ would be much sharper than predicted for an ideal two-dimensional solution.

Comparison of excess free energies of mixing also sheds light on the differences between mixed monolayers of $\text{HS}(\text{CH}_2)_{11}\text{CH}_3$ and $\text{HS}(\text{CH}_2)_{21}\text{CH}_3$ adsorbed from ethanol and isooctane. The enthalpy of mixing of liquid, linear alkanes and isooctane is positive, but the excess free energy of mixing is small and probably negative.³⁵ On the other hand, the excess free energy of mixing of alcohols and alkanes is large and positive, due to disruption of hydrogen-bonds between alcohols, and orientation of molecules to avoid hydrophobic contacts.³⁶ Consequently, the difference between the chemical potentials of $\text{HS}(\text{CH}_2)_{21}\text{CH}_3$ and $\text{HS}(\text{CH}_2)_{11}\text{CH}_3$ is likely to be higher in ethanol than in

isooctane, resulting in a greater preference for adsorption of the longer chain from ethanol than from isooctane. The unfavorable enthalpy of mixing may also explain, in part, the apparently greater depth of the minimum in $\theta_a(\text{HD})$ observed in monolayers adsorbed from isooctane than from ethanol. We believe that changes in $\theta_a(\text{HD})$ in this system reflect changes in the extent of disorder in the surface of the monolayer. In isooctane, entropy would tend to drive the outer part of the monolayer towards the most chaotic, liquid-like state. In ethanol, the positive enthalpy of mixing and negative excess entropy of mixing of the solvent and the alkyl chains would both act in the opposite direction and favor dense clusters of the alkyl chains. Such clustering might plausibly result in higher contact angles with hexadecane.³⁷ This clustering would have to arise from a different distribution of the components in the monolayer, not merely from differences in the structure of the outer phase of the monolayer: reconstruction of the fluid outer phase upon removing the monolayer from solution is probably very rapid.

Preferential adsorption of longer chains supports thermodynamic control over the adsorption process. In these experiments the concentrations of the adsorbates in solution were sufficiently low that the adsorbates were monomeric.³³ The methyl-terminated thiols do not have strongly bound solvation shells that could affect diffusion rates. Consequently, a shorter thiol diffuses to the surface slightly faster than a longer thiol. Steric constraints to adsorption should increase with increasing chain length. Since the reactivity of the thiol group is the same for all the adsorbates, it is difficult to conceive of an adsorption mechanism that would lead to a *kinetic* preference for the longer chain. In fact, we would expect kinetics to favor adsorption of the shorter chain. Thermodynamically, cohesive interactions between hydrocarbon chains favor adsorption of the longer chains. As the difference in chain length increased (compare Figs. 3 and 8), so did the preference for adsorption of the longer chain, consistent with the greater difference in the cohesive interactions between chains in monolayers of the pure components.³⁸

The adsorption isotherms of mixtures of $\text{HS}(\text{CH}_2)_{11}\text{CH}_3$ and $\text{HS}(\text{CH}_2)_{21}\text{CH}_3$ in ethanol and isooctane were very different. There is no obvious kinetic rationale for such a difference. Thermodynamically, the greater preference for adsorption of the longer chain from ethanol is a direct consequence of the poorer solvation of hydrocarbon chains in ethanol compared to isooctane (*vide supra*).³⁹

Although the preference for the adsorption of the longer chain is most easily reconciled with predominantly thermodynamic control over the composition of the monolayer, there were indications of a kinetic component in the compositions of some of the monolayers (Fig. 13). The slow change in some systems with time -- involving incorporation of more of the long-chain component -- suggests that the composition "frozen in" after the presumptive initial equilibration was partially influenced by the large excess of the shorter chain in solution. A monolayer produced with some kinetic contribution would contain more of the shorter chain than would be present at equilibrium, and would thus slowly incorporate more of the longer chain as it moved towards thermodynamic equilibrium. The slow progress towards the equilibrium composition is consistent with the rates of displacement of the components in fully-formed monolayers by thiols in solution.⁵ It is not clear why the monolayers that contained hydroxyl groups showed time-dependent behavior whereas the methyl-terminated systems reached their limiting properties upon overnight immersion. We note that mixed monolayers of eleven-carbon thiols appeared to reach their limiting compositions after overnight immersion under comparable adsorption conditions.

Mixed monolayers do not phase-separate into macroscopic islands. The pronounced minima in the contact angles of hexadecane on mixed methyl-terminated monolayers is strong evidence against formation of large, single-component domains. If islands more than a few tens of Å across were predominant on the surface, the wetting properties of the monolayer would be determined by molecules within the islands and not

by those at the domain boundaries. Since the methyl groups in each island would be expected to be ordered and well-packed, the mixed monolayers would exhibit the wetting properties of the pure monolayers i.e. the mixed monolayers would be oleophobic (Figure 1).

The next question is: To what extent is the distribution of the components in the monolayer non-statistical? The oleophilicity of the mixed monolayers of $\text{HS}(\text{CH}_2)_{11}\text{CH}_3$ and $\text{HS}(\text{CH}_2)_{21}\text{CH}_3$ adsorbed from isooctane implies that, at least in the concentration regime around $\chi^{C12} = 0.8$, the components are dispersed and the outer part of the monolayer is disordered and liquid-like. In a liquid-like regime the docosanethiol moieties would not interact strongly with each other (particularly when in contact with the liquid from which they were adsorbed) and would therefore probably be randomly dispersed in order to maximize the entropy. Intuitively, we might expect the minimum in $\theta(\text{HD})$ to occur near $\chi^{C12} = 0.5$, the maximally mixed monolayer. The actual minimum was observed near $\chi^{C12} = 0.8$, suggesting that there may be some order in the outer part of the monolayer at lower concentrations, perhaps due to the formation of small clusters of $\text{HS}(\text{CH}_2)_{21}\text{CH}_3$. The apparent difference in the depth of the minima in $\theta(\text{HD})$ on the monolayers adsorbed from ethanol and isooctane may also have arisen from variations in the distribution of the components of the monolayer on a molecular length scale. On the other hand, the differences between the contact angles of decane and hexadecane on mixed monolayers of $\text{HS}(\text{CH}_2)_{21}\text{CH}_3$ and $\text{HS}(\text{CH}_2)_{11}\text{CH}_3$ at low χ^{C12} (vide infra) require that the $\text{HS}(\text{CH}_2)_{11}\text{CH}_3$ moieties are isolated in the monolayer: if they were clustered, selective interactions with decane would not occur.

We reiterate that entropy favors dispersion of the two components at all concentrations. In both ethanol and isooctane, enthalpy favors domains comprising only one component. A balance between these two opposing forces can result in a non-random distribution of the components within the monolayer. The formation of large, single-component domains cannot occur under thermodynamic control in the systems studied

here: the formation of a pure monolayer of one or the other component would be preferred. Phase-segregation could occur only if a non-equilibrium composition were kinetically trapped, with subsequent lateral diffusion leading to the formation of islands on the surface. We believe, however, that the monolayers do reach, or at least approach, thermodynamic equilibrium before exchange between the monolayer and the solution becomes so slow that the composition of the monolayer is kinetically trapped.

A full understanding of the contact angles on mixed methyl/methylene surfaces probably requires consideration of the microscopic roughness of the surface and the entropy of mixing at the monolayer-liquid interface, in addition to dispersive interactions between the phases. (1) Structure of the monolayers. The contact angles of hydrocarbon liquids on monolayers comprising two methyl-terminated thiols with different chain lengths suggest that the outer part of these monolayers are at least partially disordered. Alkyl chains cannot be ordered at the monolayer-air interface without being densely packed. It is unlikely that the two components would be densely packed without forming single-component domains.⁴⁰ Since pure monolayers of long-chain, methyl-terminated thiols on gold are oleophobic ($\theta_a(\text{HD}) = 47^\circ$), each single-component domain would expose an oleophobic methyl surface. Consequently, the whole monolayer would be oleophobic, independent of composition. If the two components in mixed monolayers of methyl-terminated thiols were dispersed on a molecular scale, the surface would expose a mixture of methyl and methylene groups. As the surface became progressively more disordered, it would start to resemble a liquid, linear alkane. Since any liquid wets itself, we would expect a concomitant decrease in the contact angle of hexadecane. The contact angle of hexadecane was lower on the mixed surfaces than on the pure monolayers for all three methyl-terminated systems, confirming that the components in the monolayer were dispersed and the outer part of the monolayer was disordered. The decrease in contact angle was particularly marked on mixed monolayers of $\text{HS}(\text{CH}_2)_{11}\text{CH}_3$ and

HS(CH₂)₂₁CH₃ adsorbed from isooctane. Over a narrow range of concentration near R = 5 the hexadecane wet the monolayers. At the minimum in the contact angle, the free energy of the surface resembled that of a liquid paraffin: bicyclohexyl, a liquid with a higher surface tension ($\gamma_v = 32.4$ mN/m compared to 27.2 mN/m for hexadecane⁴¹) did not wet the surface.

(2) *Geometric mean approximation.* Fowkes has proposed a theoretical model¹² for evaluating contact angles at interfaces in which the interaction between the two phases is dominated by dispersion forces. His approach assumes that the liquid and solid interact enthalpically purely through Van der Waals interactions and that the ratio of the interfacial entropy⁴² to enthalpy is constant. Fowkes used the geometric mean approximation to express the solid-liquid free energy in terms of the liquid-vapor and solid-vapor free energies: for a purely dispersive system

$$\gamma_{sl} = \gamma_{sv} + \gamma_v - 2(\gamma_{sv}\gamma_v)^{1/2} \quad (4)$$

If γ_{sv} is known, then $\cos \theta$ can be predicted from Young's equation (eq (1)). If γ_{sv} is unknown, the geometric mean approximation predicts that, for a range of liquids, $\cos \theta$ should scale as $(\gamma_v)^{-1/2}$. This theory only incorporates entropic terms that adhere at least approximately to the geometric mean combining rule. The entropy of mixing at the monolayer-liquid interface cannot be predicted by such a theory since there is no contribution to γ_{sv} or γ_v from entropy of mixing. The contact angles of a series of structurally similar liquids with different surface tensions (e.g *n*-alkanes or *n*-alcohols) on pure methyl surfaces follow the predictions of the geometric mean approximation.³ The advancing contact angles on mixed monolayers of HS(CH₂)₁₁CH₃ / HS(CH₂)₂₁CH₃ and HS(CH₂)₁₁CH₃ / HS(CH₂)₁₅CH₃ were also self-consistent within the theory, with the exception of the contact angles of water in both systems, and the contact angles of decane on the C₂₂/C₁₂ monolayers (Figs. 7 and 8). We used the geometric mean approximation

and the advancing contact angles of hexadecane (or bicyclohexyl for the monolayers that were wet by hexadecane) to calculate γ_{sv} and γ_{sl}^{HD} on mixed monolayers of $HS(CH_2)_{21}CH_3$ and $HS(CH_2)_{11}CH_3$ adsorbed from isooctane (Figure 14).⁴³ One of the corollaries of the geometric mean approximation is that, for the systems studied here, changes in the contact angle are dominated by changes in γ_{sv} , not γ_{sl} . Hexadecane, bicyclohexyl and α -bromonaphthalene have different molecular shapes and might be expected to interact differently with the surface of the monolayer. Within the geometric mean approximation, γ_{sl} is small and always positive. Since specific interactions can only perturb γ_{sl} , such effects should not have a major influence on the measured contact angle.

(3) *Extensions to the theory of Fowkes*. The theory of Fowkes makes two implicit assumptions that are almost certainly untrue for the systems studied here. The first is that the surfaces of the monolayers are planar and hence that changes in the surface tension of the solid derive from changes in the polarizability of the surface. The second is that there is no entropy of mixing at the solid-liquid interface.

An alternative perspective on γ_{sv} , which may be more useful, is to regard the interfacial tension as fixed (since methyl and methylene groups have comparable volume polarizabilities⁴⁴) and allow the area of the exposed molecular surface to vary by incorporating a roughness factor r . In disordered, liquid-like monolayers we would expect the area of the exposed van der Waals surface to be greater than in an ordered, densely-packed methyl surface and the value of r to be correspondingly higher. The higher the value of r , the lower the contact angle.⁴⁵ If we then apply the geometric mean approximation to the true interfacial tension we obtain the same $(\gamma_{lv})^{-1/2}$ functional dependence of $\cos \theta$.

This alternative approach still does not account specifically for interfacial entropy. There are two contributions to the entropy of the solid-liquid interface that might be expected to influence the contact angles. For hexadecane on pure methyl-terminated monolayers the interfacial entropy is probably small. On a mixed monolayer, the

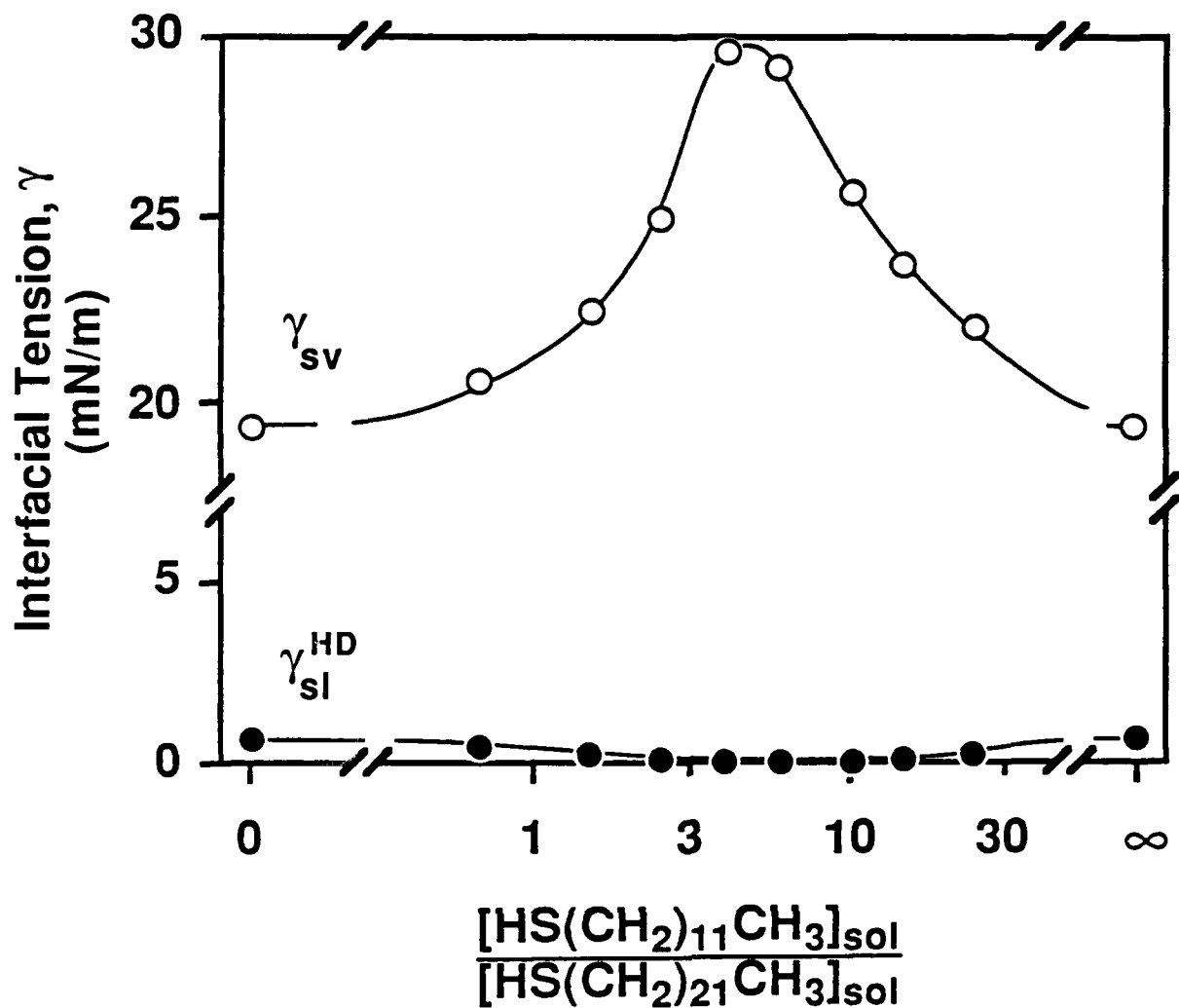


Figure 14. Interfacial tensions on mixed monolayers of $HS(CH_2)_{21}CH_3$ and $HS(CH_2)_{11}CH_3$ adsorbed from isooctane, calculated using the geometric mean approximation. Solid symbols: interfacial tension between the surface and hexadecane. Open symbols: surface tension of monolayer calculated from the contact angles of bicyclohexyl ($R=4, 6$) and hexadecane (other data points).

hexadecane dissolves in the liquid-like outer part of the monolayer, giving rise to a combinatorial contribution to the entropy. An increase in the number of conformations energetically accessible to the chains on the surface increases the conformational entropy of the interface. These entropic contributions could be of comparable size to the observed changes in surface free energies: for example, $N_A k \ln 2$ (the molar entropy of mixing of equal quantities of two ideal liquids) converts to a surface free energy of 14 mN/m at room temperature. If the entropy of mixing is important then, contrary to the model of Fowkes, changes in γ_{sl} play a major role in determining changes in the contact angle.⁴⁶ A corollary of including entropy terms in γ_{sl} is that γ_{sl} would become negative on many of the mixed monolayers.⁴⁷

(4) *Shape-selective interaction between the monolayer and the solvent.* The shape of the decane molecule approximately matches the vacancies created in a monolayer of $\text{HS}(\text{CH}_2)_{21}\text{CH}_3$ by the incorporation of $\text{HS}(\text{CH}_2)_{11}\text{CH}_3$. If molecules of decane were to fill in these holes, the resulting surface would approximate a pure methyl surface. On mixed monolayers of $\text{HS}(\text{CH}_2)_{11}\text{CH}_3$ and $\text{HS}(\text{CH}_2)_{15}\text{CH}_3$ (Fig. 8), the contact angles of decane followed the pattern expected on the basis of the contact angles of hexadecane and the respective surface tensions. On mixed monolayers of $\text{HS}(\text{CH}_2)_{11}\text{CH}_3$ and $\text{HS}(\text{CH}_2)_{21}\text{CH}_3$, however, the contact angles of decane deviated markedly from the prediction of the geometric mean approximation. As R increased and $\theta_a(\text{HD})$ decreased, the contact angle of decane initially did not change (Fig. 7). This behavior is shown graphically in Figure 15 which plots $\{\cos \theta[\text{decane}(R)] - \cos \theta[\text{decane}(R = 0)]\}$ against the corresponding change in the contact angles of hexadecane. The filled circles represent data obtained when R was less than the value that yielded the minimum in the contact angle of hexadecane, and were derived from several experiments. Data with R greater than this minimum point are shown by open circles. For most data in this regime the contact angle of decane was zero and these points are not included in the figure: the two valid data points fall on the same line as the data from the mixed monolayers of $\text{HS}(\text{CH}_2)_{11}\text{CH}_3$ and

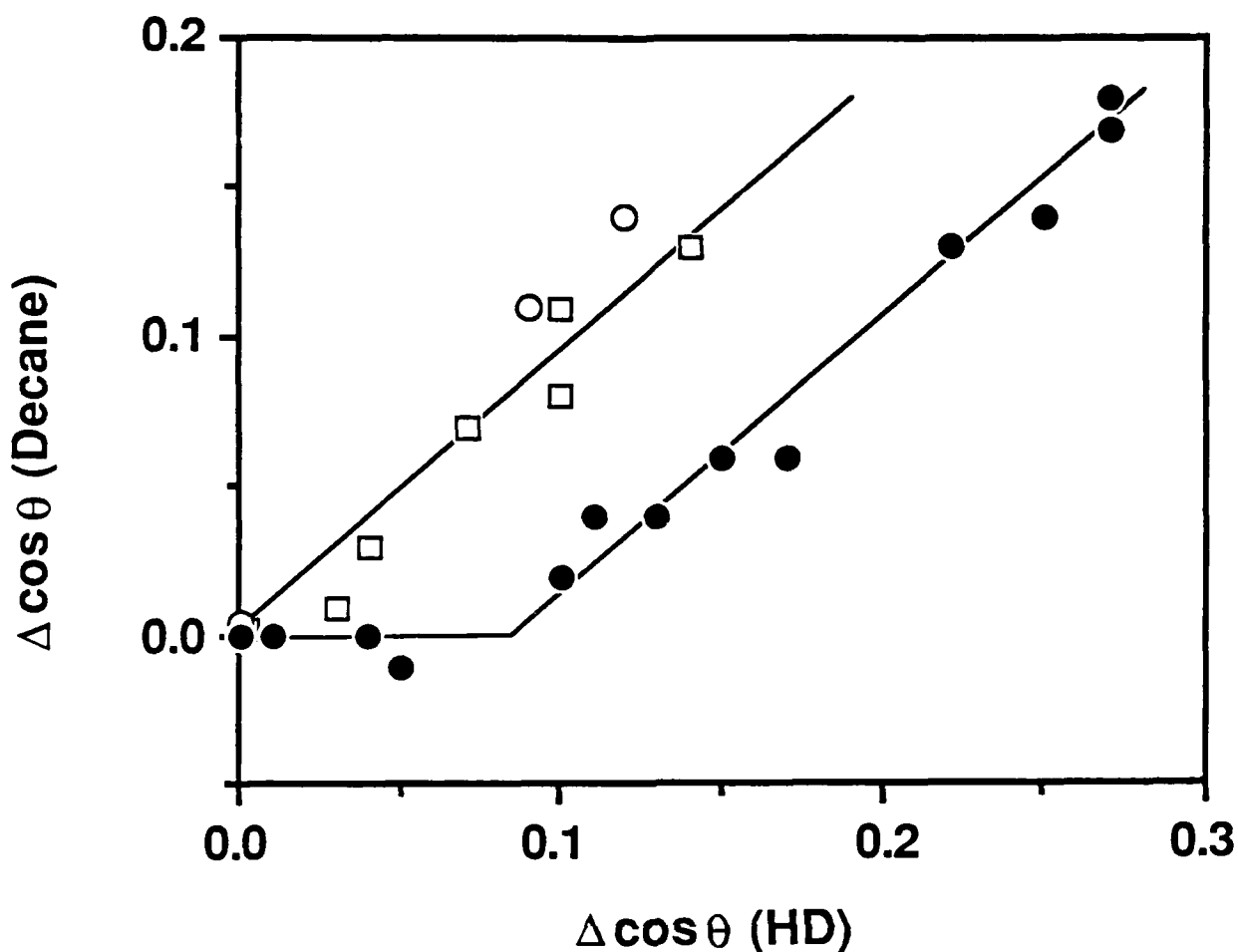


Figure 15. Changes in the advancing contact angles of decane and hexadecane on mixed monolayers of methyl-terminated alkanethiols. $\Delta \cos \theta = (\cos \theta \text{ at composition } R) - (\cos \theta \text{ at } R = 0)$. Filled circles represent data for monolayers adsorbed from mixed solutions of $\text{HS}(\text{CH}_2)_{11}\text{CH}_3$ and $\text{HS}(\text{CH}_2)_{21}\text{CH}_3$ in ethanol and isooctane, in which the contact angles were decreasing with increasing ratio of $\text{HS}(\text{CH}_2)_{11}\text{CH}_3$ to $\text{HS}(\text{CH}_2)_{21}\text{CH}_3$ in solution. Open circles represent monolayers from the same systems in which the contact angle was increasing with increasing ratio of $\text{HS}(\text{CH}_2)_{11}\text{CH}_3$ to $\text{HS}(\text{CH}_2)_{21}\text{CH}_3$ in solution. There are very few data in this range because the contact angle of decane was zero on most of these monolayers. The open squares represent monolayers adsorbed from mixed solutions of $\text{HS}(\text{CH}_2)_{15}\text{CH}_3$ and $\text{HS}(\text{CH}_2)_{11}\text{CH}_3$ in ethanol. There was no experimental difference between the two concentration regimes for this system.

HS(CH₂)₁₅CH₃ (open squares) and are in accord with the geometric mean approximation for γ_{sl} . The data represented by solid circles can be described by two intersecting straight lines. At low R, $\theta_a(\text{decane})$ did not change with decreasing $\theta_a(\text{HD})$. Once about 20% of the monolayer was composed of HS(CH₂)₁₁CH₃ moieties, $\theta_a(\text{decane})$ started to decrease: at higher R, the data followed a straight line parallel to the open symbols. The anomalous behavior of the contact angle of decane on monolayers of HS(CH₂)₂₁CH₃ admixed with some HS(CH₂)₁₁CH₃ suggests that decane was able to intercalate into voids in the monolayer. The resulting monolayers would be densely packed and would present a surface comprised essentially of methyl groups.

(5) Why might the contact angles of decane and water deviate from the theory of Fowkes? If the molecules of decane only intercalate into the monolayer at the monolayer-liquid interface, then, within the geometric mean approximation, the effect on the contact angle of incorporating decane into the mixed monolayer should be minimal, since $\gamma_{sl} \approx 0$ for decane on both a pure methyl and a disordered methyl/methylene surface. In order to explain the observed plateau in $\theta(\text{HD})$ at low R, the decane would also have to penetrate into voids at the monolayer-vapor interface. The contact angles of decane were measured under dry spreading conditions, so it is unlikely that the decane was incorporated into the monolayer before the drop was placed on the surface.⁴⁸ One could explain the observed data if a precursor film extended beyond the edge of the advancing drop. Molecules of decane in this film could penetrate into holes in the monolayer, with the energy of this process being dispersed in the advancing film. Precursor films have, however, only been established for the case $\theta_a = 0$, a condition that does not hold here.¹⁴

The contact angles of decane can be understood if the solid-liquid interfacial entropy plays an important role in the lowering of γ_{sl} on the mixed monolayers. If molecules of decane plug the holes in the monolayers of HS(CH₂)₂₁CH₃, and essentially become a part of the monolayer, then there is no entropy of mixing between the densely-packed mixed monolayer incorporating decane and the supernatant decane, and hence no change in the

equilibrium contact angle. The question of how the energy of reaction (for the insertion of molecules of decane into the monolayer) is dissipated remains unclear.⁴⁹

The advancing contact angle of water was remarkably insensitive to variations in the structure of the surfaces of the mixed monolayers of methyl-terminated thiols. Fowkes's theory, based on the assumption that the liquid and solid interact enthalpically through dispersive forces alone, predicts a maximum range of 9° in the contact angle of water⁵⁰ on the monolayers adsorbed from $\text{HS}(\text{CH}_2)_{11}\text{CH}_3/\text{HS}(\text{CH}_2)_{21}\text{CH}_3$ in isooctane, compared to the $3\text{--}4^\circ$ range observed in the advancing contact angle. There are several ways of explaining this discrepancy. First, it might be an experimental artifact. The hysteresis in the contact angle of water was higher on the mixed surfaces than on the pure monolayers (see below). Consequently, the true, equilibrium contact angle might follow the predicted behavior even though the advancing contact angle did not. Second, it might reflect microscopic roughness. Let us assume the measured contact angles are close to the thermodynamic values. Then an increase in γ_{sv} with increasing R must be matched by a corresponding *increase* in γ_{sl} . Such an increase could result from a greater area of (unfavorable) contact between the monolayer and water on mixed monolayers than on the pure monolayers. Third, it might arise from entropy of mixing. Alkanes and water are immiscible. If entropy of mixing is an important contributor to the decrease in the contact angles of hydrocarbons on the mixed monolayers, then a smaller change in θ should be observed with water since there is little entropy of mixing at the monolayer-water interface. The different positions of the minima in the contact angles on mixed monolayers of $\text{HS}(\text{CH}_2)_{11}\text{CH}_3$ and $\text{HS}(\text{CH}_2)_{21}\text{CH}_3$ (near $\chi^{\text{C}12} = 0.5$ for water, $\chi^{\text{C}12} = 0.8$ for hexadecane) demonstrate that the molecular interactions at the monolayer/water interface and the monolayer/hydrocarbon interface are different.

The hysteresis on mixed monolayers of methyl-terminated thiols is not consistent with models based on macroscopic heterogeneity. We observed some hysteresis in all the contact angles on the mixed methyl/methylene surfaces (Figure 9). For

surfaces on which the receding angle was nonzero, the hysteresis with nonpolar liquids was, with a few exceptions, essentially constant, independent of the degree of disorder in the outer part of the monolayer film. The behavior of bicyclohexyl (BCH) differed slightly from the other hydrocarbons. On the mixed monolayers adsorbed from isooctane the hysteresis in $\theta(\text{BCH})$ was not correlated with the advancing contact angle but did show variations beyond the limits of experimental error. On the monolayer adsorbed from 30:1 $\text{HS}(\text{CH}_2)_{11}\text{CH}_3/\text{HS}(\text{CH}_2)_{21}\text{CH}_3$ in ethanol, the receding edge of a drop of bicyclohexyl tended to be pinned and the resulting hysteresis was greater than on the other monolayers. The absolute size of the hysteresis of the dispersive liquids, expressed as cosines, increased with increasing surface tension. In contrast to the dispersive liquids, the advancing contact angle of water was relatively insensitive to the structure of the surface, but the hysteresis in the contact angle of water was greater on the mixed surfaces than on the pure methyl surfaces. Recalling the results from the companion paper,⁵ we can summarize our observations on hysteresis as follows:

(i) on well-packed surfaces composed of polar and non-polar components, the advancing contact angle of water is sensitive to the composition of the surface, but the hysteresis in the contact angle is constant.

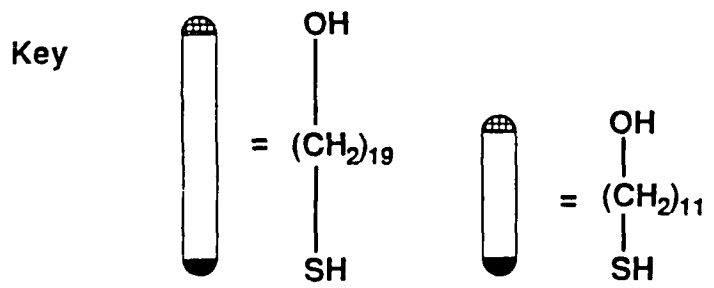
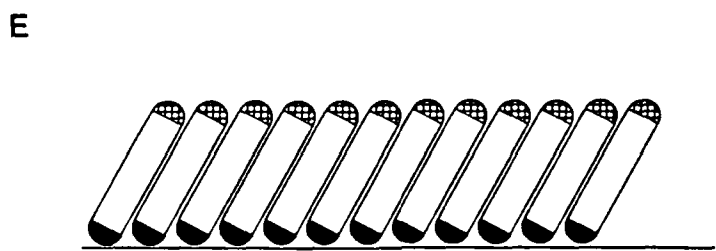
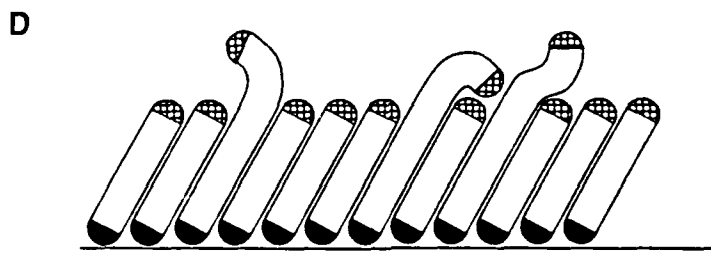
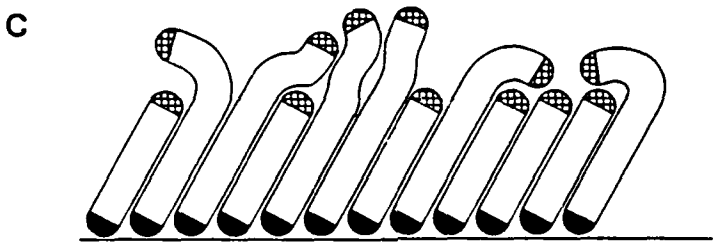
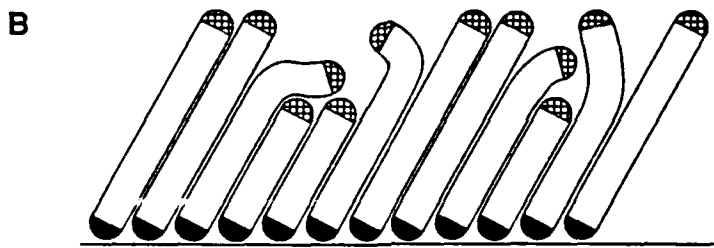
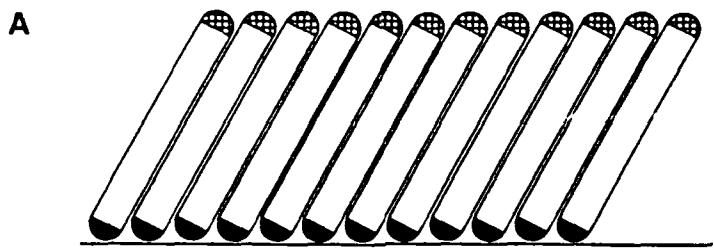
(ii) on disordered surfaces comprising methyl and methylene groups, the advancing contact angle of water is insensitive to the structure of the surface, but the hysteresis is greater on the disordered surfaces.

(iii) on disordered surfaces comprising methyl and methylene groups, the advancing contact angles of dispersive liquids are very sensitive to the structure of the surface, but the hysteresis is approximately invariant.

Current theories of wetting explain hysteresis by roughness or heterogeneity on a macroscopic scale ($\gtrsim 0.1 \mu\text{m}$).⁸ The mixed monolayers studied here are homogeneous on that length scale. It will be necessary to develop a microscopic theory to explain hysteresis in these systems.

The components in mixed monolayers of hydroxyl-terminated thiols are dispersed on a molecular scale. In light of the pronounced minimum in the contact angles of hexadecane on mixed monolayers of HS(CH₂)₁₁CH₃ and HS(CH₂)₂₁CH₃, we anticipated that we would observe a pronounced maximum in the contact angle of water on mixed monolayers of HS(CH₂)₁₁OH and HS(CH₂)₁₉OH. As Figure 10 showed, these expectations were borne out. Pure hydroxyl-terminated thiols adsorbed from ethanol onto gold and formed hydrophilic monolayers that were wetted or nearly wetted by water ($\theta_a(\text{H}_2\text{O}) < 15^\circ$ for HS(CH₂)₁₉OH; $\theta_a(\text{H}_2\text{O}) < 10^\circ$ for HS(CH₂)₁₁OH). If the two components in the monolayer were to form macroscopic islands, the resulting mixed monolayers would still be wet by water. If, however, the two components were dispersed or aggregated into small (~ a few angstroms across) clusters, then the outer part of the monolayer would become disordered and the nonpolar methylene groups of the hydrocarbon backbone would be exposed. The sharp maximum in the contact angle of water confirms the latter model. We expect the maximum in the contact angle to occur when the greatest number of methylene groups and the fewest hydroxyl groups are exposed at the surface. A monolayer composition comprising ca. 60% short chains and 40% long chains (Figure 11) is very reasonable for the maximum in contact angle. At lower R, a large proportion of the surface comprises the hydroxyl termini of the long chains, whereas at higher R there are too few hydrocarbon chains to shield effectively the hydroxyl termini of the short chains from the molecules in the water drop (Figure 16). The maximum contact angle of water is similar to that observed on a well-packed monolayer composed of ~60% hydroxyl and 40% methyl-terminated thiols.^{5,51} If we assume that the mixed monolayer with the highest contact angle ($\chi_{\text{surf}}^{\text{C11}} = 0.6$) exposes 60% hydroxyl groups and 40% methylene chains at the surface, then it is implausible that single-component clusters could be more than ~10–20 Å across.

Figure 16. Schematic illustrations of monolayers adsorbed onto gold from solutions of HS(CH₂)₁₁OH and HS(CH₂)₁₉OH in ethanol. (A) Pure monolayer of HS(CH₂)₁₉OH; (B) monolayer containing 25% HS(CH₂)₁₁OH; (C) monolayer containing 50% HS(CH₂)₁₁OH, near the maximum in contact angle; (D) monolayer containing 75% HS(CH₂)₁₁OH; (E) pure monolayer of HS(CH₂)₁₁OH.



The contact angles on mixed monolayers of HS(CH₂)₁₁OH and HS(CH₂)₂₁CH₃ suggest that the hydroxyl-terminated thiol may aggregate into small clusters when it is the minor component in the monolayer. Of all the monolayers presented in this study, the mixed monolayers of HS(CH₂)₁₁OH and HS(CH₂)₂₁CH₃ showed the most dramatic variations in composition and contact angles with the composition of the solution. Over the narrow range of R = 7 to 20, the composition of the monolayer changed from almost exclusively HS(CH₂)₂₁CH₃ to largely HS(CH₂)₁₁OH with only a few pendant chains of HS(CH₂)₂₁CH₃ extending above the surface. The energy required to bury a hydroxyl group in the nonpolar environment within a monolayer of HS(CH₂)₂₁CH₃ is probably very high (comparable to the strength of a hydrogen bond: ~5 kcal/mol) and strongly disfavors incorporation of small amounts of the hydroxyl-terminated thiol into the monolayer. In mixtures of alcohols and alkanes in solution, the alcohols are aggregated even at very low mole fractions ($\chi^{\text{OH}} \approx 0.01$).³³ By analogy, in monolayers in which the hydroxyl-terminated thiol is the minor component, the alcohol groups are probably arranged in small, internally H-bonded clusters. In monolayers composed largely of the hydroxyl-terminated thiol, the absence of cohesive interactions between hydrocarbon chains, which favor adsorption of the longer chain at lower R, result in little incorporation of HS(CH₂)₂₁CH₃ into the monolayer. We note, however, that at sufficiently low concentrations of one component in the monolayer, the combinatorial entropy of mixing (which scales as $\chi \ln \chi$) can dominate enthalpic terms (which scale as χ). The contact angles of water suggest that even at R = 200 some small amount of HS(CH₂)₂₁CH₃ was incorporated into the monolayer.

Comparison of the contact angles measured on the mixed monolayers of HS(CH₂)₁₁OH and HS(CH₂)₂₁CH₃ with those on other monolayers provide clues about the extent of aggregation of the hydroxyl-terminated chains in the monolayer. The composition of the solution that yielded an equimolar mixture of the two components on the surface ($\chi_{1/2}$) was R = 11.⁵² Consider first the contact angles of hexadecane. At $\chi_{1/2}$,

$\theta_a(\text{HD}) \approx 25^\circ$. This value is similar to the contact angle ($\theta_a(\text{HD}) \approx 30^\circ$) on a mixed monolayer of $\text{HS}(\text{CH}_2)_{21}\text{CH}_3$ and $\text{HS}(\text{CH}_2)_{11}\text{CH}_3$ at $\chi_{1/2}$, suggesting that hexadecane interacted only with the nonpolar chains of $\text{HS}(\text{CH}_2)_{21}\text{CH}_3$ and did not sense the hydroxyl groups buried below. For comparison, hexadecane wet a mixed monolayer of $\text{HS}(\text{CH}_2)_{10}\text{CH}_3$ and $\text{HS}(\text{CH}_2)_{11}\text{OH}$ at $\chi_{1/2}$.⁵

At $\chi_{1/2}$, $\theta_a(\text{H}_2\text{O}) \approx 70^\circ$. This value is much lower than the contact angle of 109° observed on the comparable monolayer adsorbed from $\text{HS}(\text{CH}_2)_{21}\text{CH}_3$ and $\text{HS}(\text{CH}_2)_{11}\text{CH}_3$ in isooctane, but higher than the angle of 50° on a mixed monolayer of $\text{HS}(\text{CH}_2)_{10}\text{CH}_3$ and $\text{HS}(\text{CH}_2)_{11}\text{OH}$ at $\chi_{1/2}$. These data suggest that water could sense the hydroxyl groups in the mixed monolayers of $\text{HS}(\text{CH}_2)_{21}\text{CH}_3$ and $\text{HS}(\text{CH}_2)_{11}\text{OH}$, but that the alcohols were shielded somewhat from the water by the hydrocarbon chains of the docosanethiol moieties. Previously we have synthesized monolayers containing polar functional groups buried within the interior of a hydrocarbon film by adsorbing unsymmetric sulfides $\text{CH}_3(\text{CH}_2)_n\text{S}(\text{CH}_2)_{10}\text{CO}_2\text{H}$ onto gold.⁵³ In these monolayers the tail groups are unable to separate into discrete polar and nonpolar phases. The contact angle of water on a monolayer of $\text{CH}_3(\text{CH}_2)_{21}\text{S}(\text{CH}_2)_{10}\text{CO}_2\text{H}$, in which a long methyl-terminated alkyl chain buries the polar carboxylic acid, was $\theta_a(\text{H}_2\text{O}) \approx 100^\circ$: water barely sensed the presence of the polar functional group. We infer that the hydroxyl groups were more accessible to the supernatant water in mixed monolayers of $\text{HS}(\text{CH}_2)_{21}\text{CH}_3$ and $\text{HS}(\text{CH}_2)_{11}\text{OH}$ than were the carboxylic acid groups in the monolayer of the unsymmetric sulfide. At lower values of R , the water still sensed the hydroxyl groups in mixed monolayers of $\text{HS}(\text{CH}_2)_{21}\text{CH}_3$ and $\text{HS}(\text{CH}_2)_{11}\text{OH}$: e.g. at $R = 8$ the monolayer contained about 30% hydroxyl-terminated chains and had a contact angle with water of 101° , similar to the mixed sulfide but still lower than the mixed monolayers of methyl-terminated thiols. A structure comprising small, internally H-bonded clusters of hydroxyl-terminated chains in a sea of disordered, methylene chains is consistent with these data. Such clusters would be accessible to fingers of water penetrating into the monolayer, but must be sufficiently

small that they can be shielded from the hexadecane by the hydrocarbon chains of adjacent docosanethiol moieties. We note that in previous studies of monolayers of ω -mercaptoethers on gold, water sensed the polar groups at greater depths below the surface than did hexadecane.²²

If the two components did form small clusters on the surface, some effect might be evident in the hysteresis in the contact angle of water. After the slides had been immersed in the adsorption solutions for 10 days, we measured the maximum advancing and minimum receding contact angles of water and remeasured the advancing contact angles of water (Fig. 13). The difference between the maximum advancing and minimum receding contact angles was much greater on the mixed monolayers than on the pure methyl surface. Similar behavior was also observed on mixed methyl-terminated monolayers, so this increase in hysteresis may just be a consequence of disorder in the polymethylene chains, or it may reflect some other aspect of the structure. Unfortunately, our understanding of hysteresis is not sufficiently complete to interpret fully data such as these.

Figure 13 also shows the contact angles of glycerol on the mixed monolayers of $\text{HS}(\text{CH}_2)_{21}\text{CH}_3$ and $\text{HS}(\text{CH}_2)_{11}\text{OH}$. Glycerol, like water, forms strong H-bonds with alcohols but its larger size limits its ability to penetrate into small crevices in the monolayer in order to reach hydroxyl groups buried beneath the surface. The advancing contact angle of glycerol at low R was less than that of water. As R increased the contact angle of water dropped faster than that of glycerol, so that at intermediate R glycerol exhibited the higher contact angle. At higher R the contact angles of the two liquids converge as both wet the pure hydroxyl surface. These data suggest that glycerol was able to sense the hydroxyl groups but may have interacted less strongly with them than water did. This interpretation would be consistent with the hydroxyl groups being isolated or in small clusters but would not support the existence of domains more than a few angstroms across.

It may not be possible to form monolayers containing isolated alcohols (or another protic functional group) in a nonpolar environment under thermodynamic control. There are

alternative approaches to this problem. For example, an alcohol group could be generated by a chemical reaction after assembly of the monolayer.⁵⁴ Alternatively, one could use monolayers that are more likely to assemble under kinetic control, such as alkyltrichlorosilanes on silicon. The range of functional groups that are compatible with trichlorosilanes is, however, much smaller than for thiols.

Contact angles are more sensitive than optical ellipsometry or X-ray photoelectron spectroscopy to certain small structural changes in monolayers. In monolayers in which the two components have the same chain length, ellipsometry is not a useful probe of the composition of the monolayer. Contact angles are sensitive to the composition so long as the wettability of the two tail groups is different, but are in general a non-linear function of the composition of the monolayer and cannot be used for quantitation. XPS is the only one of the three techniques that provides a quantitative measure of the composition of these systems. The sensitivity of XPS is comparable to that of contact angles when the component carrying the XPS tag is at low concentration. At higher concentrations, the errors in the acquisition and processing of the XPS data reduce the accuracy of the compositions and hence the ability to discriminate between two monolayers that differ slightly in composition.⁵⁵ For most of the systems studied in the preceding paper the sensitivity of the contact angle to changes in composition also decreased at high χ^P .

In monolayers containing two thiols with different chain lengths, the errors in XPS (particularly in the C/Au ratio) are less than in ellipsometry so more precise compositions can be calculated. Greater approximations are made in the analysis of the XPS data, however, which reduce the accuracy of the computed compositions. If one of the tail groups contains a heteroatom (or the tail groups contain different heteroatoms) the intensity of the photoelectrons from the heteroatom provides another estimate of composition. In these monolayers with mixed chain lengths, contact angles can detect subtle variations in

the monolayer that are buried deep in the noise in ellipsometric measurements or X-ray photoelectron spectra. Two examples illustrate this point. The contact angle of hexadecane on monolayers adsorbed from a solution of $\text{HS}(\text{CH}_2)_{21}\text{CH}_3$ and $\text{HS}(\text{CH}_2)_{11}\text{CH}_3$ in isooctane at $R = 100$ was 43° compared to 47° on the monolayer adsorbed from pure $\text{HS}(\text{CH}_2)_{11}\text{CH}_3$. At the same value of R , mixed monolayers of $\text{HS}(\text{CH}_2)_{21}\text{CH}_3$ and $\text{HS}(\text{CH}_2)_{11}\text{OH}$ yielded a contact angle of water of 14° compared to 7° on the pure hydroxyl-terminated monolayer. In neither case could we detect any significant difference by XPS or ellipsometry between the monolayers at $R = 100$ and $R = \infty$.

Conclusions

1) Mixed monolayers of thiols on gold containing two components of different chain length provide a convenient means of constructing interfaces with a controlled degree of disorder. The structure of the interface can be varied further by changing the nature of the tail groups or by introducing functional groups into the hydrocarbon chains that form the backbone of the monolayer.

2) The composition of monolayers adsorbed from solutions containing mixtures of thiols appears to be determined largely by thermodynamics, although the mechanism by which the components in the monolayer and in solution equilibrate remains unclear. There are numerous pieces of evidence in this and the preceding paper that suggest that the components in the monolayers are at, or near, thermodynamic equilibrium with the adsorption solutions at some stage during the adsorption process. Among the most compelling observations are the preferential adsorption of longer chains over shorter chains; the dramatic variation in the composition of the monolayer with the nature of the solvent, even when there are no specific interactions between the adsorbates and the solvent; and the strong preference for the adsorption of the minor component from a solution containing two structurally-similar thiols ($\text{HS}(\text{CH}_2)_{10}\text{CH}_3 + \text{HS}(\text{CH}_2)_{11}\text{OH}$ in

isooctane).⁵⁶ Since there is no reason why the rate of reaction of a physisorbed thiol with the gold surface, presumably to give a surface thiolate, should depend on the chain length or tail group, it is difficult to construct a kinetic rationale for these observations.

In contrast to the shorter chains studied in the preceding paper,⁵ some of the systems incorporating longer chains showed a kinetic component in their compositions. The initial compositions of monolayers containing hydroxyl-terminated chains comprised more of the shorter chain than would be present at thermodynamic equilibrium with the adsorption solutions. With time, more of the longer chain was slowly incorporated by displacement of the components of the monolayer by thiols in solution.

The relationships between the compositions of monolayers and the solutions from which they are adsorbed are non-ideal. Monolayers containing comparable amounts of the two components are disfavored relative to monolayers composed largely of a single-component. The adsorption isotherms can be understood qualitatively on the assumption of thermodynamic equilibrium between the monolayer and the adsorption solution, and consideration of excess enthalpies and entropies of mixing.

3) The components in the monolayer do not phase segregate into macroscopic islands. Any clusters that do form are no more than a few tens of angstroms across. It is unlikely, however, that the two components are randomly dispersed throughout the monolayer. There is some evidence for aggregation on a molecular length scale, but it is difficult to derive a detailed picture of the distribution of the two components in the monolayer.

4) We attempted to model the wettability of the mixed monolayers of $\text{HS}(\text{CH}_2)_{11}\text{CH}_3$ and $\text{HS}(\text{CH}_2)_n\text{CH}_3$ by the approach of Fowkes, who employed the geometric mean approximation to estimate the solid-liquid interfacial free energy. Although reasonable agreement was found for hexadecane, bicyclohexyl and α -bromonaphthalene, there were significant differences between the theoretical predictions and the observed contact angles of water and decane. Fowkes's model applies to planar interfaces in which

there is no entropy of mixing between the solid and the liquid. We believe that a detailed model of the wettability of these mixed monolayers must incorporate entropy. The relative importance of enthalpic and entropic terms, and how best to incorporate entropy into a coherent theory remain unclear.

5) One of the more surprising aspects of the data on mixed monolayers was the manner in which the hysteresis in the contact angle varied with the nature of the probe liquid and the structure of the monolayers. These variations cannot be understood on the basis of macroscopic heterogeneity, since no such heterogeneity exists in these systems. We feel that hysteresis contains much information about the structure of the surface, but, in the absence of a microscopic theory, we can only interpret hysteresis by comparison of a number of different systems.

Acknowledgement. We are grateful to our colleagues J. Evall and M. Chaudhury for their valuable suggestions and comments.

References and Notes

- ¹ Supported in part by the ONR and by DARPA. The XPS was provided by DARPA through the University Research Initiative, and is housed in the Harvard University Materials Research Laboratory (an NSF-supported laboratory).
- ² IBM Pre-Doctoral Fellow in Physical Chemistry 1985-86.
- ³ Bain, C. D.; Troughton, E. B.; Tao, Y.-T.; Evall, J.; Whitesides, G. M.; Nuzzo, R. G. *J. Am. Chem. Soc.*, in press.
- ⁴ Nuzzo, R. G.; Allara, D. L. *J. Am. Chem. Soc.* **1983**, *105*, 4481-4483; Porter, M. D.; Bright, T. B.; Allara, D. L.; Chidsey, C. E. D. *J. Am. Chem. Soc.* **1987**, *109*, 3559-3568.
- ⁵ Bain, C. D.; Evall, J.; Whitesides, G. M., this issue.
- ⁶ Bain, C. D.; Whitesides, G. M. *Science (Washington, D. C.)* **1988**, *240*, 62-63.
- ⁷ Bain, C. D.; Whitesides, G. M. *J. Am. Chem. Soc.* **1988**, *110*, 3665-3666.
- ⁸ For a discussion of excess thermodynamic functions, see ref. 32.
- ⁹ Nuzzo, R. G., private communication.
- ¹⁰ Experiments are in progress to determine whether there is any disorder in the inner part of the monolayer adjacent to the gold surface. In Langmuir-Blodgett monolayers of alcohols with different chain lengths, the area per molecule was found to be slightly greater than that expected on the basis of the areas per molecule in monolayers of the two pure alcohols. This discrepancy was interpreted as arising from disorder extending partially into the inner phase (Shah, D. O.; Shiao, S. Y. In *Monolayers*; Goddard, E. D., Ed.; Advances in Chemistry Series 144; American Chemical Society: Washington, DC, 1975; pp 153-164).
- ¹¹ Johnson, R. E.; Dettre, R. H.; *J. Phys. Chem.* **1964**, *68*, 1744-1750; Schwartz, L. W.; Garoff, S. *Langmuir* **1985**, *1*, 219-230; Schwartz, L. W.; Garoff, S. *J. Colloid Interface Sci.* **1985**, *106*, 422-437; Pomeau, Y.; Vannimenus, J. *J. Colloid Interface Sci.* **1985**,

104, 477-488.

¹² Fowkes, F. M. *Ind. Eng. Chem.* **1964**, *56*(12), 40-52.

¹³ Girifalco, L. A.; Good, R. J. *J. Phys. Chem.* **1957**, *61*, 904-909.

¹⁴ De Gennes, P. G. *Rev. Mod. Phys.* **1985**, *57*, 827-863.

¹⁵ Yamamura, K.; Hatakeyama, H.; Naka, K.; Tabushi, I.; Kurihara, K. *J. Chem. Soc. Chem. Comm.* **1988**, 79-81; Rubenstein, I.; Steinberg, S.; Tor, Y.; Shanzer, A.; Sagiv, J. *Nature* **1988**, *332*, 426-429.

¹⁶ Xu, H.; Huang, C. *Biochemistry* **1987**, *26*, 1036-1043.

¹⁷ Lamb, R. J.; Pecsok, R. L. *Physicochemical Applications of Gas Chromatography*; Wiley-Interscience: New York, 1978; *Chromatographic Chiral Separations*; Zief, M.; Crane, L. J., Eds.; Marcel Dekker: New York, 1988.

¹⁸ Tabor, D.; Winterton, R. H. S. *Proc. Roy. Soc. London Ser. A* **1969**, *312*, 435-?; Israelachvili, J. N. *Acc. Chem. Res.* **1987**, *20*, 415-421; Israelachvili, J. N.; McGuiggan, P. M. *Science (Washington, D. C.)* **1988**, *241*, 795-800.

¹⁹ Hallmark, V. M.; Chiang, S.; Rabolt, J. F.; Swalen, J. D.; Wilson, R. J. *Phys. Rev. Lett.* **1987**, *59*, 2879-2882; Chidsey, C. E. D.; Loiacono, D. N.; Sleater, T.; Nakahara, S. *Surf. Sci.* **1988**, *200*, 45-66.

²⁰ $\theta_a(\text{H}_2\text{O}) = 95^\circ$ for dihexadecyldimethylammonium acetate on mica (Pashley, R. M.; McGuiggan, P. M.; Ninham, B. W.; Evans, D. F. *Science (Washington D.C.)* **1985**, *229*, 1088-1089; Christenson, H. K. *J. Phys. Chem.* **1986**, *90*, 4-6).

²¹ The problem of measuring the spacing between two opaque substrates can be avoided by using gold films sufficiently thin to transmit light, or by changing to another technique, such as capacitance, for determining the separation of the two plates.

²² Bain, C. D.; Whitesides, G. M. *J. Am. Chem. Soc.* **1988**, *110*, 5897-5898.

²³ Bain, C. D.; Biebuyck, H. A.; Whitesides, G. M., submitted for publication in

Langmuir.

²⁴ Young, T. *Phil. Trans. Roy. Soc. (London)* **1805**, *95*, 65-87.

²⁵ The maximum advancing and minimum receding contact angles are defined as the angles between the surface and the tangent to the drop at the three-phase line for a drop advancing or retreating quasistatically over a motionless surface. The advancing contact angles reported in this paper were obtained under controlled conditions in which the drop advanced rapidly over the surface, and the contact angles were measured after the drop had come to rest. For a more detailed discussion, see ref. 3.

²⁶ Bartell, L. S.; Betts, J. F. *J. Phys. Chem.* **1960**, *64*, 1075-76.

²⁷ Bain, C. D.; Whitesides, G. M. *J. Phys. Chem.*, in press.

²⁸ After immersion for 1 day, the ellipsometric thicknesses yielded lower mole fractions of HS(CH₂)₁₁CH₃ in the monolayer than did the XPS data, due in large part to the anomalously low thicknesses obtained for the pure monolayer of HS(CH₂)₂₁CH₃ (compare with Figures 1 and 2). After 10 days' immersion, the agreement between the compositions calculated from XPS and ellipsometry was much better.

²⁹ In this experiment the minimum in the contact angles occurred at a slightly different value of R compared to the experiment shown in Fig. 3. This difference probably arises from inaccuracies in the preparation of the stock solution of HS(CH₂)₂₁CH₃.

³⁰ Nonane would actually fit better than decane in holes in the mixed monolayer, but the surface tension of nonane is inconveniently low.

³¹ This system is the only one in which we observed large differences between the advancing and maximum advancing contact angles. For hydrocarbons on mixed methyl-terminated monolayers the difference was less than 2°. The maximum advancing contact angle of water on the mixed methyl-terminated monolayers adsorbed from isooctane was ~ 115°, independent of composition. Sample contact angles on the mixed hydroxyl-

terminated monolayers suggested that the difference between advancing and maximum advancing contact angles in that system was $< 5^\circ$.

³² Rowlinson, J. S. *Liquids and Liquid Mixtures*; Butterworth: London, 1969; Chapters 4 and 5.

³³ Costas, M.; Patterson, D. *J. Chem. Soc. Faraday Trans. I* **1985**, *81*, 635–654.

³⁴ Ref. 32, p 162–165.

³⁵ Larkin, J. A.; Fenby, D. V.; Gilman, T. S.; Scott, R. L. *J. Phys. Chem.* **1966**, *70*, 1959–1963; McGlashan, M. L.; Morcom, K. W.; Williamson, A. G. *Trans. Faraday Soc.* **1961**, *57*, 601–610.

³⁶ Brown, I.; Fock, W.; Smith, F. *Aust. J. Chem.* **1964**, *17*, 1106–1118.

³⁷ The differences observed between monolayers with the same average composition suggests that lateral mobility in fully-formed monolayers is low. If lateral mobility were high, all the monolayers would reconstruct to the same structure in the time it took to measure contact angles.

³⁸ The preference for adsorption of the longer chain mimics the increase in the thermal stability of monolayers of alkanethiols on gold with chain length.

³⁹ The shape of the adsorption isotherms is also unusual for kinetic control of the adsorption process. Steric hindrance to adsorption is greater for the longer chain than the shorter chain, and is more important in thicker monolayers than in thinner monolayers. Adsorption of the longer chain would thus be slower (relative to the shorter chain) in monolayers comprised largely of the longer chain than in monolayers comprised largely of the shorter chain. Consequently, the adsorption isotherm would be broader than that expected if the relative rates of adsorption of the two components were constant. The actual isotherms all showed more abrupt changes in composition than predicted ideally.

⁴⁰ We have no evidence for hairpin looping of the longer component in any monolayers of

thiols on gold (Figure 1F). The strong S–Au interaction makes such loops energetically unfavorable with respect to incorporation of additional molecules of thiol into the monolayer. The one system in which loops are likely — α,ω -dithiols — appeared to be highly disordered.³

⁴¹ Jasper, J. J. *J. Phys. Chem. Ref. Data* **1972**, *1*, 841–1009.

⁴² Good, R. J. *J. Phys. Chem.* **1957**, *61*, 810–813; Fowkes, F. M. In *Surfaces and Interfaces, I — Chemical and Physical Characteristics*; Burke, Reed, Weiss, Eds.; Syracuse University Press: Syracuse, N.Y., 1967.

⁴³ We note an interesting coincidence. The value of γ_{sv} calculated on the least oleophobic monolayer adsorbed from mixtures of $\text{HS}(\text{CH}_2)_{11}\text{CH}_3$ and $\text{HS}(\text{CH}_2)_{16}\text{CH}_3$ was 22 mN/m, the same as the surface tension of octane. Both octane and the liquid-like, outer phase of the monolayer have one methyl group for each 3 methylenes. Similarly, the advancing contact angle of bicyclohexyl (25°) on the mixed monolayer adsorbed from a 4:1 ratio of $\text{HS}(\text{CH}_2)_{11}\text{CH}_3$ to $\text{HS}(\text{CH}_2)_{21}\text{CH}_3$ in isooctane, yielded $\gamma_{sv} = 30$ mN/m. This value is approximately equal to the surface tension extrapolated for eicosane (if it were liquid), which, like the disordered part of the monolayer, has one methyl group per 9 methylenes.

⁴⁴ The molecular polarizability of a linear alkane with n carbons is given approximately by $10^{24}\alpha = 4.6 + 1.8(n - 2) \text{ cm}^3$. After compensation for the different molar volumes, the polarizability of a methyl and a methylene group are comparable. (Hill, N. E.; Vaughan, W. E.; Price, A. H.; Davies, M. *Dielectric Properties and Molecular Behavior*; Van Nostrand Reinhold: London, 1969; p 192.

⁴⁵ Wenzel, R. N. *Ind. Eng. Chem.* **1936**, *28*, 988-994.

⁴⁶ A positive term due to ΔH^{mix} also contributes to the interfacial tension. For hydrocarbons on hydrocarbon surfaces ΔH^{mix} is likely to be much smaller than ΔS^{mix} .

⁴⁷One way of testing the hypothesis that part of the changes observed in the contact angles on mixed methyl/methylene surfaces is due to entropy of mixing is to measure contact angles with a dispersive liquid that is immiscible with hydrocarbons. The closest we could approach this experiment was to measure contact angles with perfluorodecalin. The free energy of mixing of fluorocarbons and hydrocarbons is much lower (i.e. less negative) than of two hydrocarbons. For example, the consolute temperature of heptane/fluoroheptane mixtures is 50 °C (Scott, R. L. *J. Phys. Chem.* **1958**, *62*, 136–145). The results of this experiment were inconclusive. We note that the geometric mean approximation predicts that perfluorodecalin ($\gamma_{lv} = 18.3$ mN/m) should wet even a pure methyl-terminated monolayer ($\gamma_{sv} = 19.3$ mN/m).³ The advancing contact angle of perfluorodecalin on a monolayer of docosanthiol on gold was 39°, and the receding contact angle was 34°. The failure of the geometric mean approximation for fluorocarbon–hydrocarbon mixtures is well-known (Scott, R. L. *op. cit.*).

⁴⁸ The contact angle of hexadecane on the monolayer adsorbed from isooctane with $R = 1.5$ was unaffected by the presence of a partial pressure of decane vapor.

⁴⁹ It is not clear how best to incorporate the energy of reaction into the theory of reactive spreading. Experiments on the ionization of carboxylic acids at interfaces suggest that the energy of reaction may influence the contact angle in some systems but not in others: Holmes-Farley, S. R.; Bain, C. D.; Whitesides, G. M. *Langmuir* **1988**, *4*, 921–937.

⁵⁰ This value was calculated from the values of γ_{sv} in Figure 14, with $\gamma(\text{H}_2\text{O}) = 72$ mN/m and $\gamma^d(\text{H}_2\text{O}) = 21$ mN/m.

⁵¹ Bain, C. D.; Whitesides, G. M. *J. Am. Chem. Soc.* **1988**, *110*, 6560–6561.

⁵² The midpoint in the ellipsometric thickness occurred at $R = 11$. The XPS data gave a value of $R = 10$ – 12 at $\chi_{1/2}$ if we assumed that the two components were dispersed, or $R = 11$ – 12.5 if the two components were separated into single-component islands.

⁵³ Troughton, E. B.; Bain, C. D.; Whitesides, G. M.; Nuzzo, R. G.; Allara, D. L.; Porter, M. D. *Langmuir*, **1988**, *4*, 365-385.

⁵⁴ Netzer, L.; Iscovici, R.; Sagiv, J. *Thin Solid Films* **1983**, *99*, 235-241.

⁵⁵ Near monolayer coverage of the molecule containing the elemental tag, the error in compositions calculated by XPS is ~5%. The lower limit on the concentration of a species that can be quantitated by XPS depends on the species being studied. For example, by tagging alcohols at the surface of a monolayer with trifluoroacetate groups it should be possible to detect 1% of a monolayer of hydroxyl-terminated thiols.

⁵⁶ HS(CH₂)₁₀CH₃ and HS(CH₂)₁₁OH have similar sizes, shapes and polarizabilities. At low concentrations in isooctane, H-bonding does not play an important role.

⁵⁷ Dettre, R. H.; Johnson, R. E. *J. Phys. Chem.* **1965**, *69*, 1507-1515.

Figure Captions

Figure 1. Schematic illustration of monolayers of thiols on gold. (A) Pure monolayer of docosanethiol. (B) Mixed monolayer of docosanethiol and dodecanethiol near the composition that yielded the lowest contact angles with hexadecane. (C) Pure monolayer of dodecanethiol. (D), (E), (F) Structures that we believe do not occur in the monolayers studied here. (D) Mixtures of docosanethiol and dodecanethiol phase-separated into islands that have the properties of the pure monolayers are not consistent with the observed contact angles. (E) An oriented monolayer with the two components dispersed on a molecular scale is unstable relative to (B). (F) Hairpin loops in the thiol with the longer chain are energetically unstable with respect to incorporation of additional molecules of a thiol into the monolayer.

Figure 2. Ellipsometric thicknesses of monolayers adsorbed onto gold from 1 mM solutions in ethanol containing a 1:1 mixture of $\text{HS}(\text{CH}_2)_{21}\text{CH}_3$ and $\text{HS}(\text{CH}_2)_{n-1}\text{CH}_3$. The dotted line represents the thickness expected if the composition of the monolayer and the solution were the same.

Figure 3. Monolayers adsorbed onto gold from ethanolic solutions containing mixtures of $\text{HS}(\text{CH}_2)_{21}\text{CH}_3$ and $\text{HS}(\text{CH}_2)_{11}\text{CH}_3$: ellipsometric thickness (upper figure) and advancing contact angle of hexadecane (lower figure) are plotted against the ratio of $\text{HS}(\text{CH}_2)_{11}\text{CH}_3$ to $\text{HS}(\text{CH}_2)_{21}\text{CH}_3$ in solution. The line in the lower figure has been added as an aid to the eye; we cannot determine from these data alone the depth of the minimum in $\theta_a(\text{HD})$.

Figure 4. Monolayers adsorbed onto gold from mixed solutions of HS(CH₂)₂₁CH₃ and HS(CH₂)₁₁CH₃ in isooctane. The abscissa represents the ratio of concentrations in solution on a logarithmic scale. Upper figure: ellipsometric thickness. Middle figure: intensity of the C(1s) (filled symbols) and Au(4f_{7/2}) photoelectron peaks (open symbols) in XPS. The areas of the gold peaks have been rescaled for clarity of presentation. The squares and circles represent two separate series of samples. The samples within each series were loaded into the spectrometer simultaneously and run sequentially. Lower figure: advancing contact angles of water (open circles), bicyclohexyl (squares) and hexadecane (filled circles). The lines have been added as aids to the eye and have no theoretical significance.

Figure 5. Ratio of C(1s) to Au(4f_{7/2}) peak areas in XPS for monolayers adsorbed onto gold from solutions of HS(CH₂)₂₁CH₃ and HS(CH₂)₁₁CH₃ in isooctane. The right-hand axis shows the equivalent chain length, *n*, of a pure monolayer of HS(CH₂)_{*n*-1}CH₃, adsorbed from ethanol, that yields the same ratio of C/Au. The scatter in the data gives an indication of the random errors. The dotted line represents the ratio of C/Au peak areas expected theoretically if $[C_{22}]_{\text{surf}}[C_{12}]_{\text{sol}}/[C_{12}]_{\text{surf}}[C_{22}]_{\text{sol}} = 2.3$.

Figure 6. Advancing contact angles of water (open circles) and hexadecane (filled circles) plotted against the mole fraction of HS(CH₂)₁₁CH₃ in a monolayer adsorbed from mixtures of HS(CH₂)₂₁CH₃ and HS(CH₂)₁₁CH₃ in isooctane. The mole fraction of HS(CH₂)₁₁CH₃ in the monolayer was calculated from the XPS data shown in Figure 5. The errors in the contact angles are within the symbols.

Figure 7. Advancing contact angles of water (), α -bromonaphthalene (), bicyclohexyl (), hexadecane () and decane () on mixed monolayers of $\text{HS}(\text{CH}_2)_{21}\text{CH}_3$ and $\text{HS}(\text{CH}_2)_{11}\text{CH}_3$ adsorbed onto gold from ethanol. The lines are provided only as an aid to the eye.

Figure 8. Ellipsometric thickness (upper figure) and advancing contact angles (lower figure) of mixed monolayers of $\text{HS}(\text{CH}_2)_{15}\text{CH}_3$ and $\text{HS}(\text{CH}_2)_{11}\text{CH}_3$ adsorbed onto gold from ethanol: water (), α -bromonaphthalene (), bicyclohexyl (), hexadecane () and decane ().

Figure 9. Hysteresis in the contact angles on mixed methyl-terminated monolayers on gold. Upper Figure: $\text{HS}(\text{CH}_2)_{21}\text{CH}_3$ and $\text{HS}(\text{CH}_2)_{11}\text{CH}_3$ adsorbed from ethanol. Middle Figure: $\text{HS}(\text{CH}_2)_{15}\text{CH}_3$ and $\text{HS}(\text{CH}_2)_{11}\text{CH}_3$ adsorbed from ethanol. Lower Figure: $\text{HS}(\text{CH}_2)_{21}\text{CH}_3$ and $\text{HS}(\text{CH}_2)_{11}\text{CH}_3$ adsorbed from isooctane. $\Delta \cos \theta = \cos$ ine of the minimum receding contact angle minus cosine of the advancing contact angle. Lines have been added to these graphs purely as aids to the eye. The variation in the hysteresis in the contact angle of bicyclohexyl in the middle figure may be significant, or may simply arise from random errors. Estimated limits of error are shown in the lower figure.

Figure 10. Mixed monolayers of $\text{HS}(\text{CH}_2)_{11}\text{OH}$ and $\text{HS}(\text{CH}_2)_{19}\text{OH}$ adsorbed onto gold from ethanol: ellipsometric thickness (upper figure) and advancing contact angles of water (lower figure) as a function of the concentrations in solution. The lower figure includes additional data, in the region of the peak maximum, that are not shown in the upper figure. The dotted line in the upper figure represents the thickness expected theoretically if $[\text{C}_{19}]_{\text{surf}}[\text{C}_{11}]_{\text{sol}}/[\text{C}_{11}]_{\text{surf}}[\text{C}_{19}]_{\text{sol}} = 5$. The solid line in the lower figure is included as an aid to the eye.

Figure 11. Advancing contact angles of water on mixed monolayers of HS(CH₂)₁₁OH and HS(CH₂)₁₉OH on gold, plotted against the mole fraction of HS(CH₂)₁₁OH in the monolayer. The composition of the monolayer was calculated from the ellipsometric thicknesses. The standard error bars were estimated from the differences in ellipsometric thickness between the monolayers on pairs of gold slides immersed in the same solutions.

Figure 12. Competitive adsorption of HS(CH₂)₁₁OH and HS(CH₂)₂₁CH₃ from solution in ethanol onto gold. Squares and circles represent two separate experiments. Upper figure: ellipsometric thickness. The dotted line represents the thickness expected theoretically, using the experimental thicknesses for the pure monolayers, if $[C_{22}]_{\text{surf}}[C_{11}]_{\text{sol}}/[C_{11}]_{\text{surf}}[C_{22}]_{\text{sol}} = 11$. Middle figure: areas of the O(1s) and Au(4f_{7/2}) peaks in the XPS spectra. Lower figure: advancing contact angles of water and hexadecane. Each symbol represents two data points. With one exception, the variation in contact angle lay within the size of the symbol on the graph: an error bar is shown to indicate the difference in contact angles for the single exception.

Figure 13. Contact angles on mixed monolayers of $\text{HS}(\text{CH}_2)_{11}\text{OH}$ and $\text{HS}(\text{CH}_2)_{21}\text{CH}_3$ measured after immersion of the gold slides in the adsorption solutions for ten days. The filled circles represent the advancing contact angles of water measured by forming a drop at the end of a needle, lowering the drop to the surface, and removing the needle. The solid line shows the values of the advancing contact angle of water on the same slides after they had only been immersed in the adsorption solutions overnight (from Fig. 12). The solid bars indicate the values of the maximum advancing and minimum receding contact angles of water, measured by the technique of Dettre and Johnson.⁵⁷ The open circles represent the advancing contact angles of glycerol, also measured after 10 days. Glycerol was used to probe the accessibility of the hydroxyl groups to an H-bonding liquid that is more sterically hindered than water. The drops of glycerol were left for several minutes on the surface before the contact angles were measured to ensure that the limiting contact angles had been reached.

Figure 14. Interfacial tensions of mixed monolayers of $\text{HS}(\text{CH}_2)_{21}\text{CH}_3$ and $\text{HS}(\text{CH}_2)_{11}\text{CH}_3$ adsorbed from isooctane, calculated using the geometric mean approximation. Filled symbols: interfacial tension between the surface and hexadecane. Open symbols: surface tension of monolayer calculated from the contact angles of bicyclohexyl ($R=4, 6$) and hexadecane (other data points).

Figure 15. Changes in the advancing contact angles of decane and hexadecane on mixed monolayers of methyl-terminated alkanethiols. $\Delta \cos \theta = (\cos \theta \text{ at composition } R) - (\cos \theta \text{ at } R = 0)$. Filled circles represent data for monolayers adsorbed from mixed solutions of $\text{HS}(\text{CH}_2)_{11}\text{CH}_3$ and $\text{HS}(\text{CH}_2)_{21}\text{CH}_3$ in ethanol and isooctane, in which the contact angles were decreasing with increasing ratio of $\text{HS}(\text{CH}_2)_{11}\text{CH}_3$ to $\text{HS}(\text{CH}_2)_{21}\text{CH}_3$ in solution. Open circles represent monolayers from the same systems in which the contact angle was increasing with increasing ratio of $\text{HS}(\text{CH}_2)_{11}\text{CH}_3$ to $\text{HS}(\text{CH}_2)_{21}\text{CH}_3$ in solution. There are very few data in this range because the contact angle of decane was zero on most of these monolayers. The open squares represent monolayers adsorbed from mixed solutions of $\text{HS}(\text{CH}_2)_{15}\text{CH}_3$ and $\text{HS}(\text{CH}_2)_{11}\text{CH}_3$ in ethanol. There was no experimental difference between the two concentration regimes for this system.

Figure 16. Schematic illustrations of monolayers adsorbed onto gold from solutions of $\text{HS}(\text{CH}_2)_{11}\text{OH}$ and $\text{HS}(\text{CH}_2)_{19}\text{OH}$ in ethanol. (A) Pure monolayer of $\text{HS}(\text{CH}_2)_{19}\text{OH}$; (B) monolayer containing 25% $\text{HS}(\text{CH}_2)_{11}\text{OH}$; (C) monolayer containing 50% $\text{HS}(\text{CH}_2)_{11}\text{OH}$, near the maximum in contact angle; (D) monolayer containing 75% $\text{HS}(\text{CH}_2)_{11}\text{OH}$; (E) pure monolayer of $\text{HS}(\text{CH}_2)_{11}\text{OH}$.

TECHNICAL REPORT DISTRIBUTION LIST, GENERAL

	<u>No. Copies</u>		<u>No. Copies</u>
Office of Naval Research Chemistry Division, Code 1113 800 North Quincy Street Arlington, VA 22217-5000	3	Dr. Ronald L. Atkins Chemistry Division (Code 385) Naval Weapons Center China Lake, CA 93555-6001	1
Commanding Officer Naval Weapons Support Center Attn: Dr. Bernard E. Doua Crane, IN 47522-5050	1	Chief of Naval Research Special Assistant for Marine Corps Matters Code OOMC 800 North Quincy Street Arlington, VA 22217-5000	1
Dr. Richard W. Drisko Naval Civil Engineering Laboratory Code L52 Port Hueneme, California 93043	1	Dr. Bernadette Eichinger Naval Ship Systems Engineering Station Code 053 Philadelphia Naval Base Philadelphia, PA 19112	1
Defense Technical Information Center Building 5, Cameron Station Alexandria, Virginia 22314	2 <u>high quality</u>	Dr. Sachio Yamamoto Naval Ocean Systems Center Code 52 San Diego, CA 92152-5000	1
David Taylor Research Center Dr. Eugene C. Fischer Annapolis, MD 21402-5067	1	David Taylor Research Center Dr. Harold H. Singerman Annapolis, MD 21402-5067 ATTN: Code 283	1
Dr. James S. Murday Chemistry Division, Code 6100 Naval Research Laboratory Washington, D.C. 20375-5000	1		

POLYMER PROGRAM DISTRIBUTION LIST

Dr. J. M. Augl
Naval Surface Weapons Center
White Oak, MD 20910

Dr. A. S. Abhiraman
School of Chemical Engineering
Georgia Institute of Technology
Atlanta, GA 30332

4132033

Dr. Harry R. Allcock
Department of Chemistry
Pennsylvania State University
University Park, PA 16802

Dr. Chris W. Allen
Department of Chemistry
University of Vermont
Burlington, VT 05405

4132007

413c012

Dr. Ronald D. Archer
Department of Chemistry
University of Massachusetts
Amherst, MA 01003

Dr. Ali S. Argon
Mechanical Engineering Department
Massachusetts Institute of Technology
Cambridge, MA 02139

413c028

a400005df

Dr. William J. Bailey
Department of Chemistry
University of Maryland
College Park, MD 20742

Dr. Kurt Baum
Fluorochem, Inc.
680 S. Ayon Avenue
Azusa, CA 91702

413a006

4000021sbi

Dr. Frank D. Blum
Department of Chemistry
University of Missouri - Rolla
Rolla, MO 65401

Dr. Len J. Buckley
Naval Air Development Center
Code 6063
Warminster, PA 18974

413m005

Dr. F. James Boerio
Materials Science & Engineering Dept.
University of Cincinnati
Cincinnati, Ohio 45221

Dr. Ivan Caplan
DTNSRDC Annapolis
Code 0125
Annapolis, MD 21401

413m012

Dr. Robert E. Cohen
Department of Chemical Engineering
Massachusetts Institute of Technology
Cambridge, MA 02139

4132001

Dr. E. Fischer
DTNSRDC Code 2853
Annapolis, MD 21402

Dr. Curtis W. Frank
Department of Chemical Engineering
Stanford University
Stanford, CA 94305

413h005

Dr. Gregory S. Girolami
School of Chemical Sciences
University of Illinois
Urbana-Champaign, IL 61801

4132014

Dr. Robert H. Grubbs
Department of Chemistry
California Institute of Technology
Pasadena, CA 91124

4132019

Dr. James F. Haw
Department of Chemistry
Texas A&M University
College Station, TX 77843

413c039

Dr. Stuart L. Cooper
Department of Chemical Engineering
University of Wisconsin
Madison, WI 53706

4132006

Dr. Warren T. Ford
Department of Chemistry
Oklahoma State University
Stillwater, OK 74078

413h006

Dr. John K. Gillham
Department of Chemical Engineering
Princeton University
Princeton, New Jersey 08544

413c005

Dr. Bernard Gordon
Department of Polymer Science
Pennsylvania State University
University Park, PA 16802

413c025

Dr. Henry K. Hall
Department of Chemistry
University of Arizona
Tucson, AZ 85721

413j009

Dr. Alan J. Heeger
Department of Physics
University of California, Santa Barbara
Santa Barbara, CA 93106

4132012

Dr. Pat J. Hendra
Department of Chemistry
University of Southampton
Highfield Southampton 509 5NH
United Kingdom
4134001

Dr. Bruce S. Hudson
Department of Chemistry
University of Oregon
Eugene, Oregon 97403

413c018

Dr. Hatsu Ishida
Department of Macromolecular Science
Case Western Reserve University
Cleveland, OH 44106

413m008

Dr. Paul M. Lahti
Department of Chemistry
University of Massachusetts
Amherst, MA 01003

413c037

Dr. Robert W. Lenz
Polymer Science and Engineering Dept.
University of Massachusetts
Amherst, MA 01002

441c013

Dr. Alan D. MacDiarmid
Department of Chemistry
University of Pennsylvania
Philadelphia, PA 19104

a400004df

Dr. Charles E. Hoyle
Department of Polymer Science
University of Southern Mississippi
Hattiesburg, MS 39406-0076

413c026

Dr. Leonard V. Interrante
Department of Chemistry
Rensselaer Polytechnic Institute
Troy, NY 12181

413c014

Dr. Jeffrey T. Koberstein
Institute of Materials Science
University of Connecticut
Storrs, CT 06268

4132013

Dr. Richard M. Laine
Washington Technology Center
University of Washington
Seattle, WA 98195

s400033srh

Dr. Geoffrey Lindsay
Chemistry Division - Code 087
Naval Weapons Center
China Lake, CA 93555

4132036

Dr. Chris W. Macosko
Materials Science & Engineering Dept.
University of Minnesota
Minneapolis, MN 55455

4132029

Dr. Joseph H. Magill
Materials Science & Engineering Dept.
University of Pittsburgh
Pittsburgh, PA 15161

413c013

Dr. Tobin J. Marks
Department of Chemistry
Northwestern University
Evanston, IL 60201

413c030

Dr. Krzysztof Matyjaszewski
Department of Chemistry
Carnegie Mellon University
Pittsburgh, PA 15213

413j002

Dr. William B. Moniz
Code 6120
Naval Research Laboratory
Washington, DC 20375-5000

4132012

Dr. Virgil Percec
Department of Macromolecular Science
Case Western Reserve University
Cleveland, OH 44106-2699

413c024

Dr. Roger S. Porter
Dept. of Polymer Science & Engineering
University of Massachusetts
Amherst, MA 01002

413m006

Dr. Leo Mandelke
Department of Chemistry
Florida State University
Tallahassee, FL 32306-3015

4132018

Dr. Lon J. Mathias
Department of Polymer Science
University of Southern Mississippi
Hattiesburg, MS 30406-0076

413m003

Dr. James E. McGrath
Department of Chemistry
Virginia Polytechnic Institute
Blacksburg, VA 24061

4132007

Dr. Kay L. Paciorek
Ultrasystems Defense and Space, Inc.
16775 Von Karman Avenue
Irvine, CA 92714

s400029srh

Dr. Martin Pomerantz
Department of Chemistry
University of Texas at Arlington
Box 19065
Arlington, TX 76019-0065
a400008df

Dr. T. J. Reinhart, Jr.
Nonmetallic Materials Division
Air Force Materials Laboratory (AFSC)
Wright-Patterson AFB, OH 45433

Dr. Arnost Reiser
Insitute of Imaging Sciences
Polytechnic University
333 Jay Street
Brooklyn, NY 11021

4132022

Dr. Charles M. Roland
Code 6120
Naval Research Laboratory
Washington, DC 20375-5000

413m009

Dr. Ronald Salovey
Department of Chemical Engineering
University of Southern California
Los Angeles, CA 90089

413m010

Dr. Jerry I. Scheinbeim
Dept. of Mechanics & Materials Science
Rutgers University
Piscataway, NJ 08854

4132009

Dr. L. E. Sloter
Code Air 931-A
Naval Air Systems Command
Washington, D. C. 20361-9310

Dr. Dietmar Seyferth
Department of Chemistry
Massachusetts Institute of Technology
Cambridge, MA 02139

413c004

Dr. Ferdinand Rodriguez
Department of Chemical Engineering
Cornell University
Ithaca, NY 14853

413c011

Dr. Michael F. Rubner
Materials Science & Engineering Dept.
Massachusetts Institute of Technology
Cambridge, MA 02139

413m007

Dr. Jacob Schaefer
Department of Chemistry
Washington University
St. Louis, MO 63130

413m001

Dr. Lawrence R. Sita
Department of Chemistry
Carnegie Mellon University
Pittsburgh, PA 15213

4132030

Dr. Richard R. Schrock
Department of Chemistry
Massachusetts Institute of Technology
Cambridge, MA 02139

4132038

Dr. David S. Soane
Department of Chemical Engineering
University of California, Berkeley
Berkeley, CA 94720-9989

413h004

Dr. Les H. Sperling
Materials Research Center #32
Lehigh University
Bethlehem, PA 18015

413c002

Dr. C. S. Sung
Institute of Materials Science
University of Connecticut
Storrs, CT 06268

413m011

Dr. C. H. Wang
Department of Chemistry
University of Utah
Salt Lake City, Utah 84112

413c020

Dr. Robert A. Weiss
Department of Chemical Engineering
University of Connecticut
Storrs, CT 06268

a400006df

Dr. Garth L. Wilkes
Department of Chemical Engineering
Virginia Polytechnic Institute
Blacksburg, VA 24061

4132020

Dr. Richard S. Stein
Polymer Research Institute
University of Massachusetts
Amherst, MA 01002

4132008

Dr. Sukant K. Tripathy
Department of Chemistry
University of Lowell
Lowell, MA 01854

4132016

Dr. Kenneth B. Wagener
Department of Chemistry
University of Florida
Gainesville, FL 32611

a400007df

Dr. George M. Whitesides
Department of Chemistry
Harvard University
Cambridge, MA 02138

4132010